ISSN No:-2456-2165

Wave Refraction and Energy Attenuation Properties of Underwater Curved Breakwaters and Their Potential Application for Coastal Defence

Michael L. Hackett
Affiliation: Department of Mathematics, Physics and Statistics,
Faculty of Natural Sciences, University of Guyana, Tain Campus, Guyana.

Research Location: Faculty of Engineering, Science and Mathematics
School of Civil Engineering and the Environment, University of Southampton, United Kingdom.

Abstract:- An investigation was carried out to determine the energy-dissipating effects of submerged curved planform breakwaters on water waves. The submerged breakwaters are of the shape of planoconvex and planoconcave optical lenses in planform. Physical modeling involving small-scale structures in a wave tank was done.

The general concept is to make use of the refractive effects of the contours of these shapes to refract and cause converging or diverging of water waves so that they undergo superposition after passing over the shapes. When the waves superpose constructively their heights will increase according to the principle of superposition and, if the wave-breaking criteria for deep to shallow water are reached, breaking will occur and the wave energy will be dissipated in the lee of the submerged breakwaters. This will help to reduce wave impacts on coastal structures and on vulnerable shorelines by using an unobtrusive and aesthetic means of coastal protection.

The research involved measuring the wave heights of incident waves in front of the submerged structures and the wave heights of transmitted waves in the lee. In this way, the incident and transmitted wave energy density can be obtained to determine the wave transformations that may have been caused by the breakwaters. Energy loss coefficients were also computed. Comparisons were done with the wave energy transformations produced by rectangular planform submerged breakwaters of comparable size.

Generally, it was found that all three types of breakwaters dissipated wave energy, with the planoconcave ones performing the least and the rectangular ones the best. The planoconvex breakwaters performed comparably to the rectangular ones, showing only slightly smaller energy density dissipations and loss coefficients.

So, it is possible for planoconvex breakwaters to replace rectangular ones and give comparable energy attenuation performance for a lower cost and fewer building materials.

Keywords:-

- *Absolute error of measurement – half the size of the smallest graduation interval on a measuring instrument and taken as the best possible accuracy.*
- *Crest width – distance from front to back of breakwater, usually rectangular in planform.*
- *Crest freeboard – for a submerged breakwater, distance from the top of the breakwater to still water level.*
- *Platform depth – same as crest freeboard.*
- *Planform – the shape of an object as viewed from directly above it.*
- *Real focal point – point to which waves converge and meet at that point.*
- *Superposition – the crossing over of wave crests and troughs from different wave sources so that wave heights are either increased or decreased due to constructive and destructive interference.*
- *Relative error – absolute error of a measurement divided by the value of the measurement expressed as a percentage of that value: relative error = (absolute error/measured valued) × 100 %.*
- *Virtual focal point – point from which waves appear to diverge as if coming from that point.*
- *Wave series (WS) – a wave condition defined by an incident wave period and wave height as determined by the wave paddle frequency and amplitude.*

I. INTRODUCTION

A. Background to Submerged Features

➢ *Effects caused*

The effects of submerged features on surface water waves near coastal regions have always been of interest to coastal engineers. Depending on their depth, shape, permeability, and other properties, these underwater features can cause waves to change speed, direction, wavelength, and height producing the effects of shoaling, breaking, focusing, reflection, refraction, diffraction, and changes in energy density, among other phenomena (Reeve *et al*, 2004). The overall effect of a submarine feature is to change the wave field around it by its presence, whereas the wave field would have been different in the absence of the feature. Changes in the wave field between the lee of the features and the coast can produce changes in the wave impacts and loadings that natural and artificial coastal structures experience. This is of interest to the coastal engineer.

➢ *Submerged breakwaters*

One use to which submerged features have been put is in the construction of submerged breakwaters for coastal and harbour protection and to prevent beach erosion (Losada *et al*, 1996). The idea of using submerged breakwaters is to have structures that are below still water level at all times and are aesthetic and unobtrusive yet offer some protection to coastlines and coastal structures by dissipating the energy of the waves via bottom friction turbulence, breaking, reflection, and other means as they pass over the structures (Smith *et al*, 1995; Reeve *et al*, 2004). These are used in coastal areas where a high degree of protection is not required, as by traditional above-surface emerged breakwaters, and where the wave climate is generally mild, but protection against erosion and wave action is still needed (Christou *et al*, 2008).

Although submerged breakwaters do not provide full protection, they have less environmental impact than emerged breakwaters, suffer less from direct wave impacts, have less impact on natural sediment transport, promote better circulation and exchange of water between the seaward and leeward sides, and are cheaper to build and maintain. Coastal engineers are increasingly regarding them as an alternative means of coastal protection vis-à-vis the traditional emerged breakwaters (Zhu *et al*, 2002; Hung *et al*, 2008; Coastal Wiki, 2008).

➢ *Shapes of submerged breakwaters*

The usual shapes of submerged breakwaters are rectangular in planform and trapezoidal or hemispherical in vertical cross-section. T-shaped and vertical cylindrical breakwaters have also been studied. These breakwaters generally dissipate wave energy by inducing shoaling and breaking over the breakwater and in the lee when the wave height-depth limitation (H/d = 0.78) criterion for shallow water over the breakwater is exceeded (Kamphuis, 2000; Sorensen, 2006). There is also energy reduction due to bottom friction, reflection, and vortex shedding.

This investigation, however, takes a different approach in focusing on the use of curved planform submerged breakwaters, shaped like optical lenses, to dissipate wave energy by virtue of the refraction effects of their curved planform shape.

B. Genesis of Project Idea and Rationale

➢ *Alderney Breakwater and Braye Rock, Channel Island, UK.*

The question of the effects of curved planform submerged breakwaters on waves arose from the damage suffered by the Alderney Breakwater in 1992 from wave action. A submerged natural rock plateau, known as the Braye Rock, lies about 150 m in front of the Breakwater. During the 1992 event, waves passing over Braye Rock were refracted and focused, producing superposition and constructive interference of wavefronts along the sides of the Breakwater. The wave heights increased at these points, leading to increased loadings on the Breakwater which resulted in a 50-m breach (Müller, 2008).

➢ *Submerged Rock Plateaus*

Generally, submerged rock plateaus are convex or more-or-less circular in planform shape and would have a convergent focusing effect on waves passing over them, as with the Braye Rock. However, if submerged features are concave in planform the effect should be the opposite so as to cause waves to diverge and spread their energy over a larger area, leading to a dispersion, and hence reduction, of the energy. Also, if concave and convex structures can be arranged in a line parallel to incoming wave crests it may be possible to induce superposition of the waves from adjacent structures so that their heights increase, and they break and dissipate energy before reaching the coastline. The structures should therefore similarly act on water waves as optical lens act on light waves.

➢ *Rationale*

The general idea is to use the curved planform shape of the submerged breakwaters to change the wave field so that wave energy is dissipated, even partially, before reaching the shoreline. This would help to reduce wave impacts and loadings on coastal features and structures.

Also, if curved breakwaters are feasible then an immediate advantage would be a saving in the cost and materials required to build them, since, due to their curvature, they would need fewer construction materials than rectangular breakwaters of comparable sizes and efficiencies.

C. Scope and Aim of the Investigation

This investigation was conducted to determine the effects of submerged curved planform structures on the passage of waves over them. Specifically, how submerged shapes in convex and concave planforms affect the passage of water waves over them to dissipate and to converge or focus the wave energy density. The investigation used physical micro-modeling involving a wave tank, wave generator, and paddle to generate monochromatic unidirectional waves which were passed over planoconvex and planoconcave submerged structures. Wave sensors of the surface-piercing resistance-depth type were used to measure the water elevation time series at selected points around the structures and analyzed to determine changes in wave heights, wave periods, wavelengths, and wave energy density as the waves pass over the structures.

The purpose of the planoconvex and planoconcave breakwaters is to make use of the converging and diverging effects of refraction when waves move from deep to intermediate or shallow water to cause the waves to converge or diverge and to superpose. When the waves superpose their heights will increase or decrease according to the principle of superposition. If constructive superposition occurs the wave heights increase and if the breaking criterion is reached the waves will break and dissipate their energies. The wave-parallel front of the planoconvex and planoconcave shape of the breakwaters may also cause some reflection of the wave energy, thereby further reducing the energy that reaches the shore. However, the aim of this research is not to measure the reflection

caused by the front of the breakwaters but to measure the dissipation of energy in the lee of the breakwater.

At low tide, the breakwaters will still be submerged but with a smaller depth of water over them, and here the usual breaking and shoaling conditions for waves passing over them will apply. When the tide is high, then the focusing and refraction effects will come into play and cause the waves to either diverge or converge and thus undergo superposition when the crests pass over one another in the lee of the structures.

A comparison was made between rectangular-shaped submerged breakwaters and curved planform submerged breakwaters with respect to their effects on waves. The breakwaters were subjected to various wave climates comprising waves of different periods and heights.

The wave generator and paddle used a computer software programme that generated sinusoidal horizontal movement of the wave paddle which then produced parallel crest water waves in the wave tank. As recommended by Christou *et al* (2008), waves were first generated in the tank without any structure in it to record and determine the wave heights, wave periods, wavelengths, and wave energies produced to compare them with the waves in a tank that has structures placed in it.

Various arrangements and a number of structures were placed in the tank, and they were subjected to the selected wave climates, each of which used ten waves. The initial waves that were incident over the breakwaters were selected so as to be non-breaking and small-amplitude waves to meet the criteria and conditions for Airy waves and Airy equation, that is, linear or first-order wave theory (Reeve *et al*, 2004). The depth of the water used was 0.15 m and the waves generated were of the intermediate and deep-water types for relative depths $0.05 < d/L < 0.5$ and $d/L > 0.5$, respectively.

D. Structure of the Report

The remainder of this report deals with the background to the research, a review of the relevant literature, the theoretical and physical principles involved in the research, a concise description of the experimental methodology, a presentation of the results and discussion of the findings, and ending with the conclusions and recommendations of the study.

II. BACKGROUND

A. Review of Relevant Literature

Submerged breakwaters are generally able to dissipate most of the energy of waves of high steepness (H/L) in their lee while allowing waves of smaller steepness to pass with less attenuation. This is useful since the higher steepness waves are associated with coastal erosion processes, while lower steepness waves with coastal building processes (Smith *et al*, 1995). If the same or comparable efficiency of wave energy dissipation can be achieved by curved planform submerged breakwaters, then there can be a saving in building costs and construction materials due to the curvature of the structures.

To the researcher's knowledge, the use of concave or convex planform submerged breakwaters as means of coastal protection by dissipating wave energy has not been reported in the literature. Those that have been used in coastal engineering and investigated in the literature include rectangular planform submerged breakwaters and semicircular and trapezoidal vertical cross-section breakwaters.

Cho *et al* (2006) studied sinusoidal wave reflection due to trapezoidal submerged breakwaters using numerical analysis and laboratory experiments. They compared the reflection characteristics of porous breakwaters with non-porous ones and found that the porous breakwaters have smaller reflection coefficients because much of the incident energy is dissipated in the porous structure. They also found that for short waves the permeability of the structures has negligible effects on reflection, indicating that reflection is wavelength dependent.

Priya *et al* (2000) investigated the effects of submerged semicircular vertical cross-section breakwaters on reflection characteristics, hydrodynamics pressures, and forces exerted by regular waves using laboratory models. To ensure a significant measurement of reflection, they subjected their model to sixty waves.

Among their findings was that the reflection coefficient decreases as water depth over the breakwater increases, thus reflection is depth dependent.

Losada *et al* (1996) analyzed models of submerged porous rectangular breakwaters and of breakwaters with a slope, i.e., trapezoidal breakwaters, to determine the interaction of non-breaking regular waves with them. They analyzed how incident wave obliqueness, relative depth, breakwater geometry, and porosity of material affected wave reflection, transmission, and energy dissipation.

Cheng *et al* (2003) also reported the use of semicircular vertical cross-section submerged breakwaters, as well as T-shaped and vertical cylinder types. Their research focused on the latter type using one to three arrangements of cylinders that were subjected to non-breaking waves. They found that with an increasing number of cylinders, the wave field became distinctly non-linear so that linear theory was unable to describe it, instead non-linear theory worked better at describing the field.

Neelamani and Rajendran (2000) studied the use of partially submerged T-shaped breakwaters using physical models. Their breakwater consisted of a broad flat horizontal plate in the shape of the letter T and supported by piles under the foot of the T. As well as dissipating wave energy by wave breaking over the horizontal top and by friction between the waves and the top, the foot of the T induced vortex shedding which also helped to dissipate some of the wave energy. They found that the energy transmission coefficient, K_T, generally decreases with increasing wave steepness, H/L, and increasing relative depth, d/L. This, therefore, means that the energy loss coefficient, K_L, will generally increase with increasing H/L and increasing d/L.

The February 1996 issue of Engineering Research News reported on a laboratory investigation into the use of a submerged horizontal plate breakwater model. Like, the T-type, this one consisted of a submerged horizontal plate supported by piles. This breakwater reduces wave energy in the lee side by reflection seaward, breaking over its top, friction, and by vortex-shedding by flow separation above and below the plate.

McCormick (1981) discussed the use of "focusing by refraction on submerged structures having horizontal areas in the shape of optical lenses" in wave energy conversion devices. He applied the lens-maker equation from wave optics to water waves and calculated the focal distances of water waves passing over convex planform structures. He found that the focal distances were dependent on wavelength, wave celerity, and water depth over the structure.

Mehlum and Stamnes (1979) also studied the use of lens focusing by submerged lens-shaped platforms for wave energy conversion. Their idea was to focus the incoming wave energy as the waves pass over the lens-shaped submerged structure to a focal point where a wave energy conversion device was placed.

However, no reports of convex or concave planform submerged breakwaters have been found. It is hoped that the results of this study will stimulate further and more detailed research into the use of curved planform breakwaters as a means of coastal defence.

B. Hypothesis and Objectives

- *Statement of hypothesis and explanation*

The hypothesis is that curved planform submerged structures can be used for wave energy dissipation by making use of the refractive effects of the shape of the structures. When waves pass over the lens-shaped submerged structures they will undergo refraction due to the reduced depth of water over the structure and their direction will change due to the curved shape of the submerged platform. When they re-enter deeper water in the lee of the structures the wave directions will have changed so that waves coming from adjacent structures will superpose and increase their heights, then break and dissipate their energy.

By arranging a series of these structures, parallel to the wave fronts of incoming waves, it is expected that the shape of the structures, as well as the reduced depth, will cause the wavefronts to slow down and change direction as they pass over the structures. On the lee side of the structures, the wave fronts will undergo superposition when they change direction and cross over one another and their heights will increase. If the breaking criteria are reached, the waves will experience breaking and will dissipate their energies before reaching the shore or any coastal structure. Bottom friction turbulence will also dissipate some of the wave energy as the waves pass over the breakwater (Reeve *et al*, 2004).

- *Objectives*

The objectives of the study are to determine the changes in energy density caused by the selected structures and their arrangements, to evaluate the loss coefficients and upon these two bases, to say which structures and arrangement can offer good dissipation of wave energy and can be used as a means of coastal protection.

III. THEORY AND PHYSICAL PRINCIPLES INVOLVED

A. Refraction and Superposition

When plane wavefronts encounter a step change in depth, there are changes in wavelength, wave celerity, wave height, and, depending on the obliqueness of incidence, wave direction (Chaplain, 2008). Figure 1 shows how plane waves are refracted when they meet a step change in depth representing a simplified *convex* boundary while moving from shallow water to deeper water. The platform depth is d_s, that is, the crest freeboard of the submerged structure, and d is the depth in the lee side of the structure. The wave celerity over the structure and in its lee are C_2 and C_1, respectively. Therefore, $d_s < d$ and $C_2 < C_1$, and given that the waves will refract according to Snell's Law, they will change direction in the manner illustrated (*Ibid*; Kamphuis, 2000; Reeve *et al*, 2004; Sorensen, 2006).

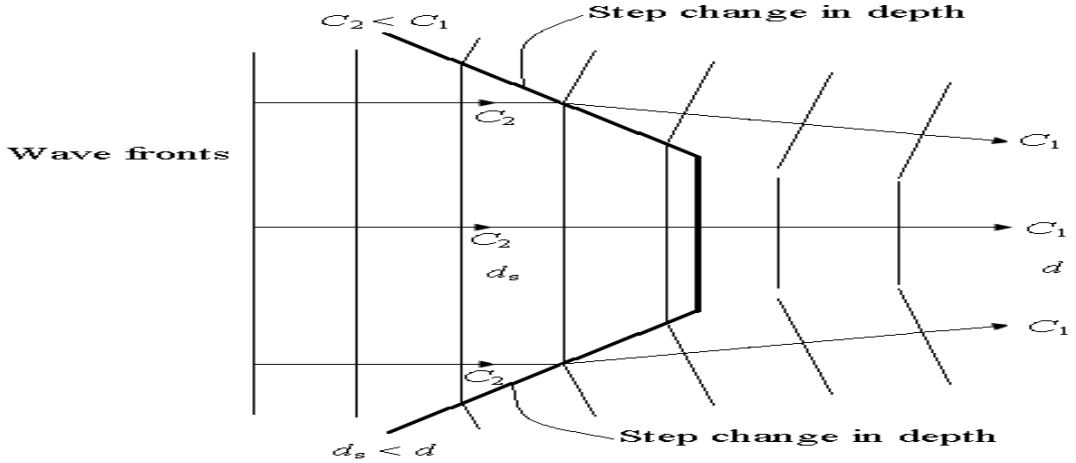

Fig. 1: Wave refraction at simplified convex boundary

ISSN No:-2456-2165

Figure 2 shows how the waves are refracted when they meet a step change in depth representing a simplified *concave* boundary while moving from shallow water to deeper water.

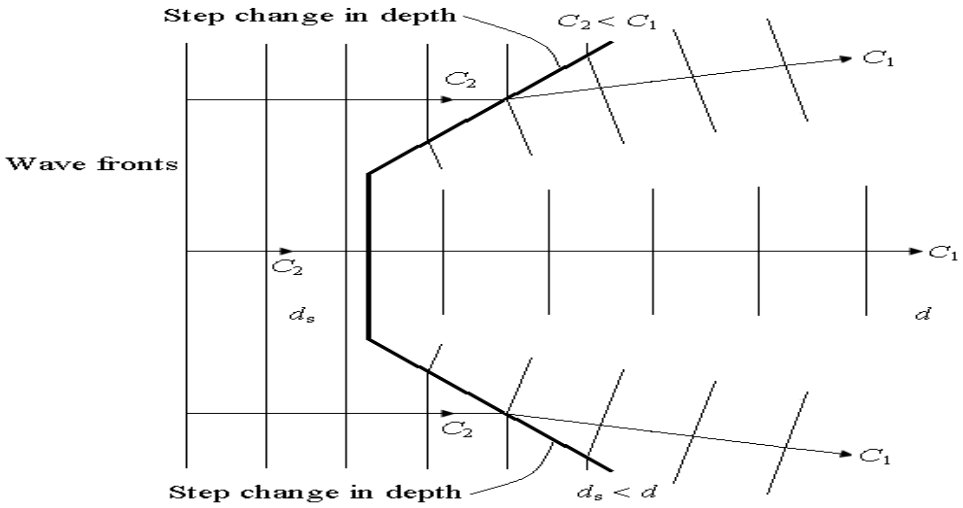

Fig. 2: Wave refraction at simplified concave boundary

When plane waves cross over a planoconvex shape they will refract and form curved wave fronts as shown in Figure 3. The waves that pass over the middle of the structure will slow down more and will reach the deep lee side after those that pass over the ends, so the ends of the wave fronts will curve outwards and the middle inwards. The waves in the lee will converge to a point called the real focal point so that the energy density there will increase.

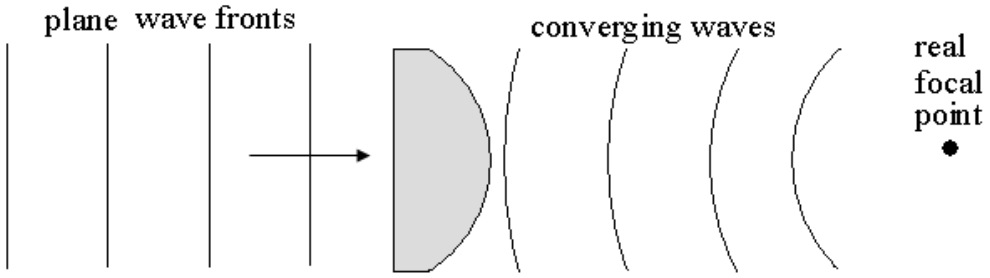

Fig. 3: Wave refraction by planoconvex shape

With the planoconcave shape, the plane waves will refract as shown in Figure 4. In this case, the waves that pass over the middle of the structure will reach the deeper lee side before those that pass over the ends of the shape and will also slow down less, so the ends of the wave fronts will curve inwards and the middle outwards in the lee. The waves diverge in the lee as if coming from a point in front of the breakwater - that point is the virtual focal point for those waves. In the lee, the wave energy density will be reduced as the waves diverge and spread out.

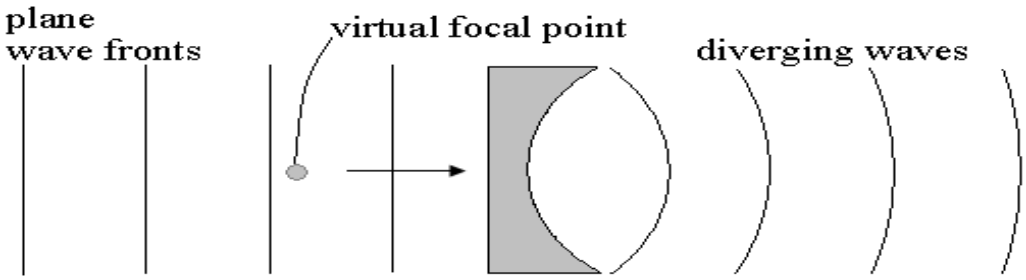

Fig. 4: Wave refraction by planoconcave shape

When two planoconcave structures or two planoconvex structures are placed adjacent to each other, with or without an intervening gap, *a*, the wave crests from each will overlap as shown in Figures 5 and 6 and superposition will occur where the waves cross over one another and the wave height will increase at the points labeled A, B, C, D, and E, among others. Breaking will occur if the breaking criteria are reached and wave energy will be dissipated. Because of multiple superpositions of waves occurring rapidly over time, the wave field in the lee might not be linear; however, the wave heights can still be measured to determine if wave energy density has increased or decreased to give an indication of the efficiency of the shapes and their arrangement in dissipating wave energy.

ISSN No:-2456-2165

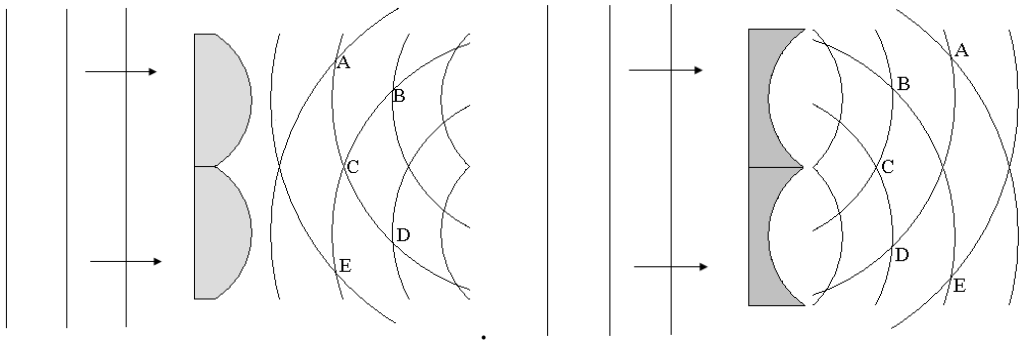

(a) (b)

Fig. 5: Wave superposition by (a) two planoconvex and (b) two planoconcave without gaps between them

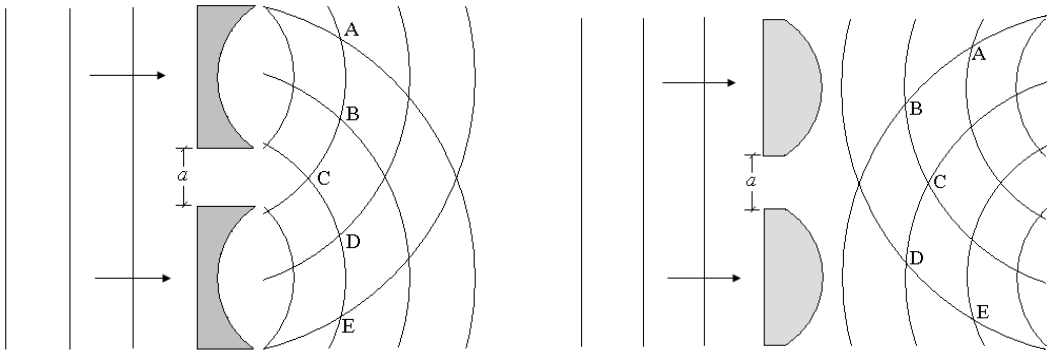

(a) (b)

Fig. 6: Wave superposition by (a) two planoconvex and (b) two planoconcave with gaps between them

More details of the passage over waves over a planoconvex submerged structure are provided in Figure 7 (adapted from McCormick, 1981). Waves traveling in deep water, depth d, with celerity C_1 and wavelength L_1, will meet the plane front of the structure and enter the shallower water, depth d_s, over it, which will cause a decrease in celerity and wavelength to C_2 and L_2, respectively. Upon re-entering deep water past the convex curvature, the wave orthogonals will converge, as shown in the diagram, and the wave fronts will refract, as described earlier, to form converging or focused waves with celerity, C_1.

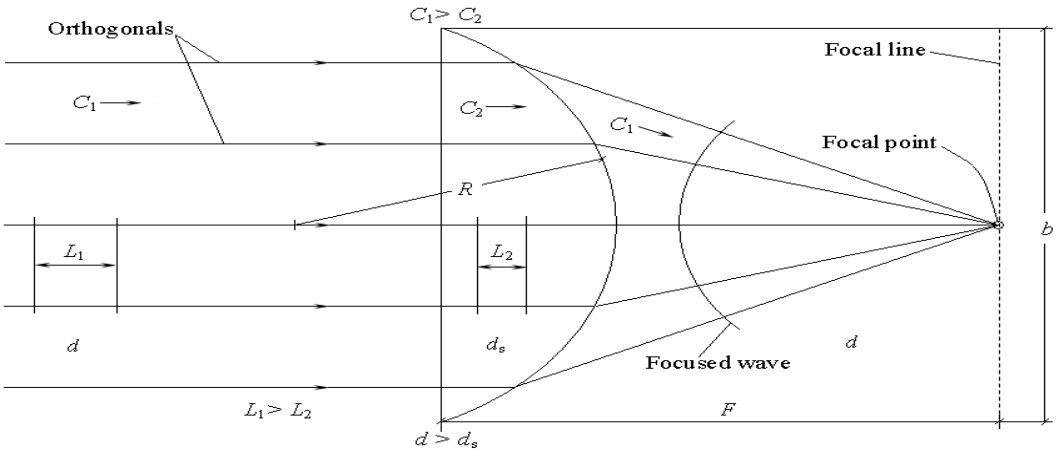

Fig. 7: Wave refraction over a planoconvex structure

The focal distance, F, is given by the lens maker equation (Nelkon, 1978; McCormick, 1981; Halliday & Resnick, 1992):

$$F = \frac{R}{(C_1/C_2)-1} \tag{3.1}$$

where R = radius of curvature of the convex face. Given that wave celerity, $C = L/T$, and that the period, T, of the waves, remains unchanged during refraction over the change of depth (Dean & Dalrymple, 1991), then the equation can be re-written as:

$$F = \frac{R}{(L_1/L_2)-1} \tag{3.2}$$

The passage of waves over a planoconcave structure is illustrated in Figure 8. The description for wave refraction is

the same as for the planoconvex structure, except that in this case, due to the concave curvature, the orthogonals will bend away from one another and the wave fronts will diverge once past the structure.

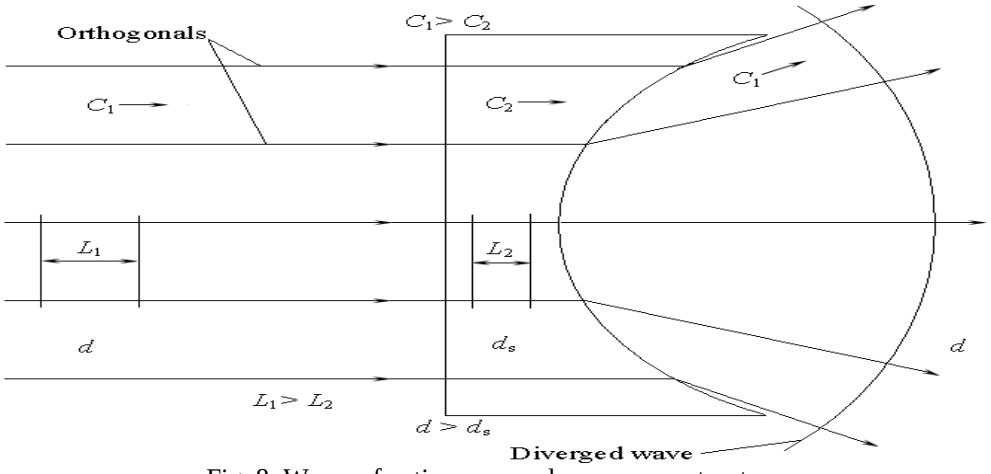

Fig. 8: Wave refraction over a planoconcave structure

Since the focal point of the planoconcave shape is virtual, that is, not a real point where waves would meet and pile up as with the planoconvex shape, there is no need to calculate a focal distance. The salient point is that the concave curvature should cause waves to diverge and disperse their energy in the lee of the structure.

B. Wave Energy and Energy Coefficients

➢ *The Law of Conservation of Energy*

Generally, from the law of conservation of energy:

Incident Energy = Reflected energy + Dissipated energy + Transmitted energy:

$$E_I = E_R + E_L + E_T \quad (3.3)$$

$$\Rightarrow \quad 1 = \frac{E_R}{E_I} + \frac{E_L}{E_I} + \frac{E_T}{E_I} \quad (3.4)$$

Now since wave energy, E, is directly proportional to the square of wave height, H, that is, $E \propto H^2$, then it follows that:

$$1 = \left(\frac{H_R}{H_I}\right)^2 + \left(\frac{H_L}{H_I}\right)^2 + \left(\frac{H_T}{H_I}\right)^2 \quad (3.5)$$

$$1 = (K_R)^2 + (K_L)^2 + (K_T)^2 \quad (3.6)$$

(Priya et al, 2000; Neelamani & Rajendran 2000)

➢ *Reflection, Transmission, and Loss Coefficients*

Reflection coefficient, $K_R = H_R/H_I$, where H_R = height of reflected wave, H_I = height of incident wave (Sorensen, 2006).

Transmission coefficient $K_T = H_T/H_I$, where H_T = height of transmitted wave, H_I = height of incident wave (Stauble & Tabar, 2003).

Loss coefficient, K_L, is defined in terms of K_R and K_T since it cannot be measured directly, as H_L is only theoretical given that the energy would have dissipated and so H_L would be non-existent.

So the dissipation or loss coefficient should be properly defined in terms of energy and not wave heights. Thus, $K_L = \sqrt{(E_L/E_I)}$. If we assume that the reflection coefficient, K_R, can be neglected, for this research, then:

$$1 = (K_L)^2 + (K_T)^2 \quad (3.7)$$

$$\Rightarrow \quad K_L = \sqrt{1-(K_T)^2} \quad (3.8)$$

Hence, knowing the wave heights, H_T, and H_I, values for K_T and K_L can be readily calculated.

From Equation 3.3, and assuming negligible E_R, then:

$$E_L = E_I - E_T \quad (3.9)$$

➢ *Percentage Energy Density Losses*

Hence, from Equation 3.9, the percentage energy loss:

$$\%E_L = \left(\frac{E_I - E_T}{E_I}\right) \times 100\% \quad (3.10)$$

Therefore, by adjusting this formula so that it gives a negative percentage for a decrease in energy density and a positive percentage for an increase in energy density, the percentage energy density *change*, indicated by the Δ symbol, can be calculated using the formula below:

$$\%\Delta E = \left(\frac{E_T - E_I}{E_I}\right) \times 100\% \quad (3.11\ a)$$

$$= \left(\frac{E_T}{E_I} - 1\right) \times 100\% \quad (3.11\ b)$$

where $\%\Delta E$ = percentage energy density change

E_I = incident energy density (from H_I measured by Probe 1)

E_T = transmitted energy density (from H_T measured by Probes 2, 3 & 4)

A negative percentage would indicate energy density dissipation or divergence and a positive percentage would indicate energy density focusing or convergence.

This would be a useful formula to compare energy density changes caused by different shapes and their arrangements. Now, from Equations 3.11 a & b:

$$\frac{\%\Delta E}{100\%} = \left(\frac{H_T}{H_I}\right)^2 - 1 \qquad (3.12)$$

$$\Rightarrow \qquad \frac{\%\Delta E}{100\%} = (K_T)^2 - 1 \qquad (3.13)$$

And from Equation 3.7:

$$(K_L)^2 = 1 - (K_T)^2 \qquad (3.14)$$

$$\Rightarrow \qquad \frac{\%\Delta E}{100\%} = -(K_L)^2 \qquad (3.15)$$

$$\Rightarrow \qquad K_L = \frac{\sqrt{-\%\Delta E}}{10} \qquad (3.16)$$

And $$\%\Delta E = -100(K_L)^2 \qquad (3.17)$$

The loss coefficient, K_L, can also be calculated from the percentage energy change, provided it has a negative value, that is, it is a decrease of energy density, and not an increase, which has a positive value.

➢ *Complex Number Values for Loss Coefficient*

An increase in energy density could happen when there is a convergence or focusing of wave energy due to superposition, and HT would be greater than HI. In such a case it is clear from Equation 3.8 that KL would not have a real number value, but a complex number value.

If the energy density increases in the lee of the structures, then there is an increase in wave height, so that KT > 1, then from Equation 3.8, KL will be a complex number of the form aj where j = √(-1) and a = a positive number. Also, from Equation 3.16, an increase in energy density will render KL as a complex number, which is meaningless in the context of this study. From Equation 3.17, a percentage decrease in energy density can be readily determined for a given loss coefficient.

In the results tables, complex values of KL are indicated by an asterisk (*), whenever they occur. Hence, only the real KL values will be considered. Average KL values will be computed for each wave condition used and an overall average KL value will be found for each type and arrangement of structure used.

A comparison of the KL values for the type and arrangement of structures used would also indicate those which yield better dissipation of wave energy. The percentage energy change would indicate the relative amount of energy dissipated.

IV. EXPERIMENTAL METHODOLOGY

A. The Experiments

➢ *Location and Time of Experiments*

The experiments for this research were conducted in Room 1017: Hydraulics Laboratory, Building 21, School of Civil Engineering and the Environment, University of Southampton during July-August 2009.

➢ *List of Apparatus Used*

- Perspex-sided wave tank 3 m long × 1.5 m wide × 0. 3 m high
- Wave generator – mains supply electric motor, wave paddle (1.48 m wide × 0.29 m high), and accessories linked to desktop computer
- Desktop computer loaded with probe calibration, wave generation, and wave data collection programmes
- Wave monitors linked to wave probes and computer
- Four wave probes – surface-piercing parallel electrodes and connecting co-axial cables
- Wave-absorbing cellular foam material
- Planoconvex, planoconcave and rectangular shapes made from Perspex/Plexiglas (density 1,190 kg/m^3).

➢ *Experimental Outline*

A small-scale Perspex wave tank of length 3.0 m, width 1.5 m, and height 0.3 m was used with a constant water depth of 0.15 m for all wave series experiments. Waves were generated by an electric motor-driven wave paddle that produced sinusoidal outputs. Triangular-shaped foam material was used at the opposite end of the wave tank as wave absorbers. Resistance-type wave probes were used to measure wave heights and wave periods. The wave probes were calibrated before each experiment to obtain a linear calibration equation of voltage versus wave amplitude. This was applied to the voltage readings obtained from the wave probes to convert them into wave height values. Data were logged from all four probes used. The probes were labeled Probes 1, 2, 3, and 4 and this labeling was used throughout the experiments and in this report.

The experimental set-up of the wave tank, paddle, probes (Pr 1, 2, 3 & 4), absorbers, and two planoconvex structures are shown in Figures 9 (a) & (b).

The planoconcave structures were placed in the same position. When only one structure was used, it was placed 1.28 m away from the paddle directly in between Probes 1 and 3. The plane front of the model faced the paddle and the curved back faced the wave absorbers.

ISSN No:-2456-2165

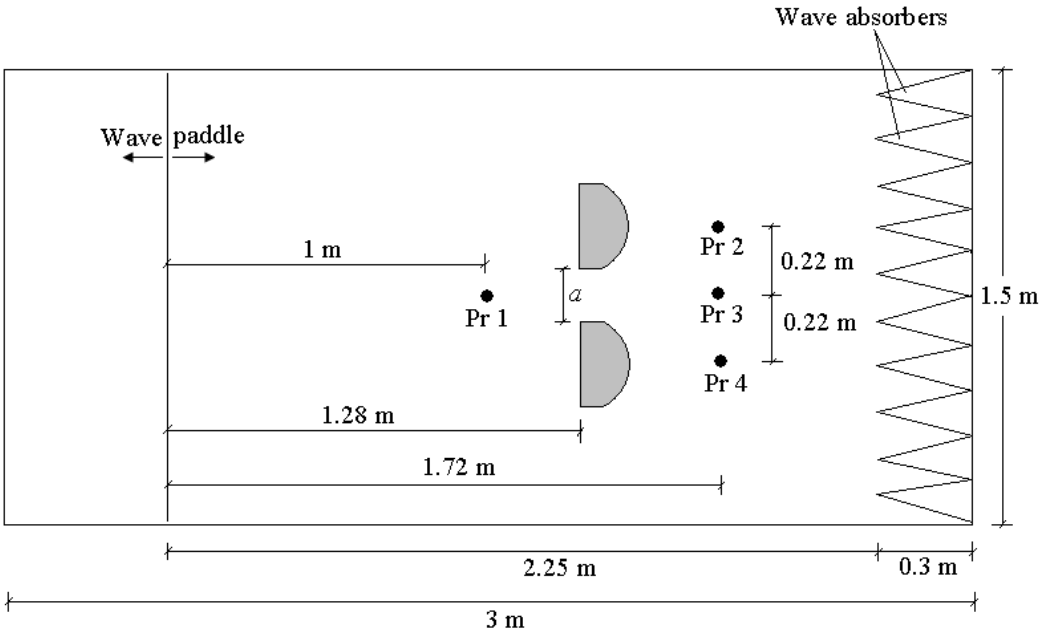

(a) Plan

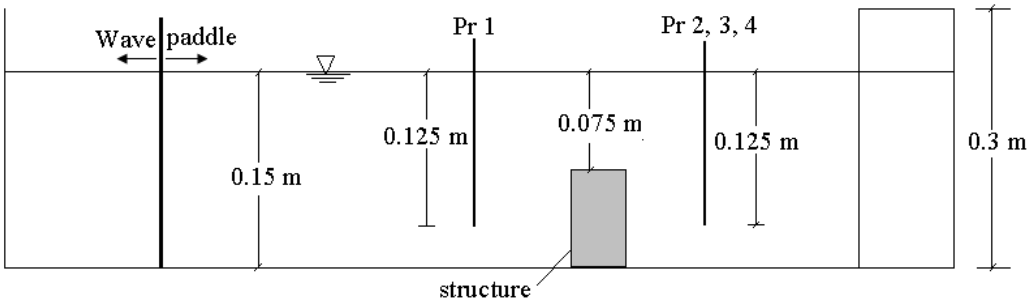

(b) Side

Fig. 9: Definition sketches of experimental set-up with one arrangement of structures

The width, *a*, of the gap between the structures was varied at three values: a = 0 cm, 7cm, and 14 cm to observe any effects on the waves of varying gap widths.

The experiments were done using twelve different wave conditions comprising four paddle frequencies and several paddle amplitudes for each experiment, shown in Table 1.

➢ *Wave Conditions Used*

Table 1: Wave conditions used for the experiments.

Paddle Output			**Theoretical**	**Theoretical**
Wave series (WS)	**Frequency, *f* (Hz)**	**Amplitude (V)**	**Wave period *1/f* = *T* (s)**	**Wavelength *L* (m)**
1	1.5	0.7	0.667	0.628
2	1.5	0.6	0.667	0.628
3	1.5	0.5	0.667	0.628
4	2.0	0.5	0.500	0.385
5	2.0	0.4	0.500	0.385
6	2.0	0.3	0.500	0.385
7	2.25	0.4	0.444	0.307
8	2.25	0.3	0.444	0.307
9	2.25	0.2	0.444	0.307
10	2.5	0.3	0.400	0.250
11	2.5	0.25	0.400	0.250
12	2.5	0.2	0.400	0.250

The paddle frequency (and period) closely approximated the frequency (and period) of the waves generated as measured by the wave probes. A run of ten waves was generated for each wave series lasting for about 10 - 12 seconds. Thus, each configuration of structures was subjected to ten waves in each wave series.

The wave series were set to run one after the other using the Batch Datataker Drive and Collect Programme with intervals of 3 – 5 minutes between each series to allow for the waves to attenuate completely and still water conditions to return before another series was started. From the wave period, the wavelength was calculated by iteration using Microsoft Excel formula function to compute the linear wave theory equation for the wavelength of water waves in intermediate depth conditions as used in the wave tank (Kamphuis, 2000; Reeve et al, 2004):

$$L = \frac{gT^2}{2\pi}\tanh\left(\frac{2\pi d}{L}\right) \quad (4.1)$$

The waves were selected to have small steepness and to be non-breaking so as to remain linear and make use of small amplitude linear theory. For all the incident waves selected, H/L < 0.12 and H/d < 0.35 in the water depth of 0.15 m.

➢ *Calculating Wave Energy Density*

The wave heights of the incoming waves were measured by Probe 1 as well as the wave heights in the lee of the submerged structures by Probes 2, 3, and 4. Using the wave energy density or energy per unit surface area equation for small-amplitude wave theory (*Ibid*; Sorensen, 2006):

$$E = \frac{\rho g H^2}{8}, \quad (4.2)$$

where

E = energy density or energy per unit surface area (in J/m^2),

ρ = density of water (1,000 kg/m^3 for freshwater used in the wave tank),

g = gravitational acceleration (9.81 m/s^2),

H = wave height (in metres),

The energy density of the incident and transmitted waves was calculated and compared to determine the changes in the energy density of the waves. A decrease in energy density is taken as a dissipation or divergence of wave energy, while an increase in energy density is taken as a focusing or convergence of wave energy.

A comparison of the energy density dissipation or increase was done for the various structures and arrangements used to see which gave the best dissipation of wave energy density, and under what wave conditions these dissipations took place. Since the focus of this research is on energy density changes in the lee of the breakwater, the reflection in front of the breakwater was not considered. In fact, due to the selected wave conditions, number of waves used per series, and the relative depth of the platform to the water depth, the reflection was considered negligible. Thus, only the incident wave energy density and the transmitted wave energy density were considered to determine changes in the energy density.

B. The Model Structures

➢ *Description*

Planoconvex, planoconcave, and rectangular planform shapes were made from 1.5 cm thick Perspex. These models were therefore non-porous and impermeable. Their shapes and dimensions, including the radius of curvature, R = 16 cm of the curved shapes are shown in Figure 10. The surface areas of their planform are: rectangular 435 cm^2 (0.0435 m^2); planoconvex 366 cm^2 (0.0366 m^2); planoconcave 243 cm^2 (0.0243 m^2).

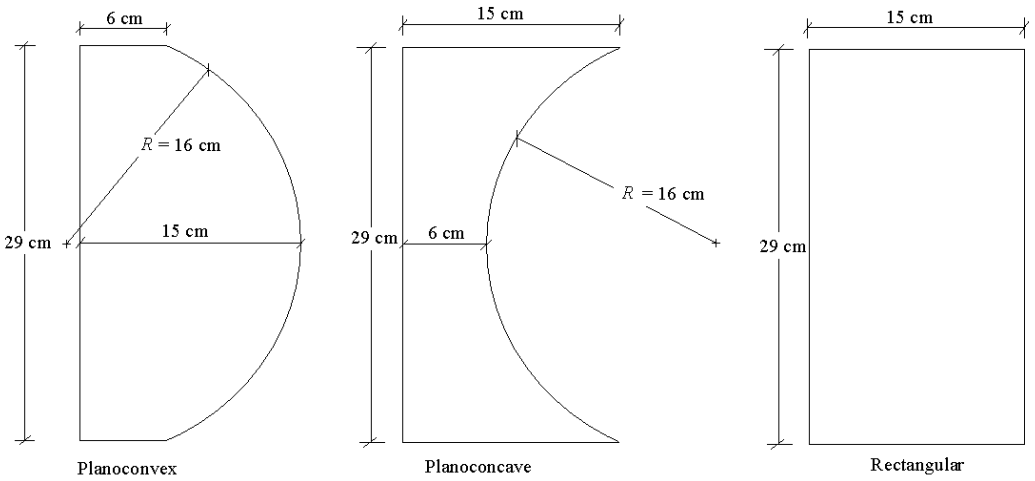

Fig. 10: Planform view of model structures

Congruent shapes were stacked on one another and bolted together to give a structure of the required height of 7.5 cm and platform depth, ds = 7.5 cm (also referred to as the crest freeboard). Hence, reflection from the plane front

of the structures can be considered negligible since the water depth, d = 15 cm, and most of the wave energy will pass over the structures to be dissipated or transmitted in the lee. The use of only ten waves for each wave series also ensured that the reflections did not amplify and so can be considered negligible.

The structures were made of comparable dimensions so that a realistic and valid comparison can be made of the effects of each on wave energy density.

➢ *Focal Distance of Planoconvex Structures*

Using Equation 3.2, the focal distances of the planoconvex model structure, platform depth, d_s = 0.075 m in tank water depth, d = 0.15 m, for the four wave frequencies (and periods) used were calculated and are shown in Table 2.

Table 2: Wavelengths and focal distances of planoconvex structure

T (s)	L_1 (m) in d = 0.15 m	L_2 (m) in d_s = 0.075 m	L_1/L_2	F (m)
0.667	0.628	0.507	1.239	0.67
0.500	0.385	0.343	1.122	1.31
0.444	0.307	0.286	1.073	2.18
0.400	0.250	0.240	1.042	3.84

The placement of the planoconvex structures in the wave tank ensured that their focal distances lay within or close to the wave absorbers or beyond the boundary of the wave tank for the given wave conditions. This prevented the waves from coming to a direct focus in the tank and interfering with the measurements of wave heights on the lee side of the structures due to dissipation or convergence of energy density. The planoconcave and rectangular structures were placed in the same position to ensure a good comparison with the planoconcave ones. It is important to note that the focal point of the planoconvex is a real point on the lee side where wave crests could meet, but the focal point of the planoconcave is a virtual or imaginary point in the seaward side where waves would only appear to diverge from after passing over the structure.

➢ *Arrangement and Type of Structures*

The type and arrangement of structures used for the investigation are given in Table 3 below. Each type and arrangement were subjected to the twelve wave conditions listed in Table 1 above.

Table 3: Types of structures and arrangements used in experiments.

Experiment	Structures	Amount	Distance between structures a (cm)
1	No structures	0	NIL
2	Planoconvex	1	NIL
3	Planoconcave	1	NIL
4	Rectangular	1	NIL
5	Planoconvex	2	0
6	Planoconcave	2	0
7	Rectangular	2	0
8	Planoconvex	2	7
9	Planoconcave	2	7
10	Rectangular	2	7
11	Planoconvex	2	14
12	Planoconcave	2	14
13	Rectangular	2	14

➢ *Shoaling coefficient and limiting wave steepness over model structures*

The shoaling coefficient, K_s, for waves passing over the structures of platform depth, d_s = 0.075 m was calculated using the shoaling equation:

$$K_s = \sqrt{\frac{1}{\left(1+\frac{4\pi d_s / L}{\sinh\left(4\pi d_s / L\right)}\right)\tanh\left(2\pi d_s / L\right)}} \quad (4.3)$$

The limiting wave steepness, H/L, at which waves would break over the structures, was calculated using the Miche formula (Kamphuis, 2000; Sorensen, 2006):

$$\frac{H}{L} = 0.142\tanh\left(\frac{2\pi d_s}{L}\right) \quad (4.4)$$

Details are given in Table 4.

Table 4 Shoaling coefficients and limiting wave steepness for waves over structures

Period T (s)	Wavelength over platform L (m)	Relative depth over platform d_s/L	Shoaling coefficient K_s	Miche Limiting Wave Steepness (H/L)
0.667	0.507	0.148	0.927	0.104
0.500	0.343	0.219	0.916	0.125
0.444	0.286	0.262	0.930	0.132
0.400	0.240	0.313	0.949	0.137

➢ *Scale of the Modeling*

The length scale used in the physical modeling was 1:100 and the corresponding time scale was 1:10. Hence, a modeled wave of period 0.5 s and length 0.385 m in the 0.15 m wave tank will scale up to a real wave of period 5 s and length 38.5 m in a depth of 15 m. Table 5 below shows the details for the modeled waves used and the full-scale waves.

Table 5: Modeled and full-scale wave details

Modeled waves in depth 0.15 m			Full-scale waves in depth 15 m		
Period (s)	Wavelength (m)	d/L	Period (s)	Wavelength (m)	d/L
0.667	0.628	0.24	6.67	62.8	0.24
0.500	0.385	0.39	5.00	38.5	0.39
0.444	0.307	0.49	4.44	30.7	0.49
0.400	0.250	0.60	4.00	25.0	0.60

So, the modeled waves used represented full-scale waves of periods 6.67 – 4.00 seconds, which are the periods generally found in mild wave conditions and are therefore taken as being representative of that period range (Sorensen 2006).

C. The Wave Probes

➢ *Calibration of Probes*

The wave probes were connected to the wave monitors and calibrated using the 32-channel data collection programme [1.01 ASCII] software. The depth of immersion of the probes has a linear relationship with the voltage across the parallel electrodes of the probe. When a wave crest passes the probe the immersion depth increases and causes the voltage across the parallel electrodes to increase proportionally. The passage of a trough causes the immersion depth to decrease, producing a proportional decrease in the voltage (Armfield Engineering Education, 2006).

All probes were set immersed to a still water depth of 12.5 cm, leaving a 2.5 cm clearance between the bottom of the tank and the tip of the probe. The still water level was taken as the datum (zero) wave amplitude, and the voltage at that water level was noted. The wave amplitude is therefore the difference between still water level and the immersion depth of the probe when a crest or trough passes. Then the probes were raised by measured steps of 1.5 cm several times and the voltage was noted each time for each level. In this way a linear graph and equation relating wave amplitude to voltage was produced – this is the calibration equation. The correlation of determination, R^2, for the calibration graphs had values between 0.999 and 1, showing the calibration graphs and equations obtained were highly accurate and linear. The probes were then re-set to the still water level (zero datum amplitude) and the measurements began.

➢ *Experimental Error Inherent in Wave Probes*

The water depth and wave probe immersion depth were measured with a metre rule during the calibration of the probes. So, the theoretical minimum absolute error of the measurements achieved by the probes would be half the smallest graduation of the metre rule, i.e., $\pm$ 0.5 mm accuracy. (Christou *et al*, 2008). However, since it was the metre rule that was used to calibrate the wave probes, and not the metre rule used to measure the wave heights during the experiments, then it would be more realistic to assume a practical error of ± 1 mm or ± 0.1 cm accuracy.

For the largest wave height of 5.1 cm measured by the probes, the relative error would be 2 %. This would translate into a relative error of 4 % in calculating wave energy density, as energy is proportional to the square of wave height, and when a measurement is squared the relative error is doubled. The smallest wave height measured was 1.5 cm. So, the associated relative errors would be 6.7 % for wave height and 13.3 % for energy density. For the loss coefficient, the relative errors will be of the same order of magnitude.

➢ *Processing Wave Probe Data*

The input wave series for the wave generator was produced by the OWEL Batch Datataker Drive and Collect Programme software and the wave data from the probes were recorded by the same programme. The raw data from each wave probe were logged as time series of voltage (in volts) against time (in seconds) in data files. These were converted into wave amplitudes (in metres) using the calibration equations for the probes.

Using Microsoft Excel Spreadsheet software, graphs of wave amplitudes against time were produced for each wave probe. From these graphs, the wave periods, T, and wave heights, H, were obtained using the filter application available in Excel to filter out spikes in the data. The

average height of the ten waves generated for each wave series was determined and that was used as representative for that particular series. It was noted that the period measured by the probes closely approximated the period of the wave paddle. The wave periods and heights were then used to calculate the wavelength using Equation 4.1 and wave energy density using Equation 4.2.

D. Limitations of the Experiments

➢ *Insufficient number of wave probes*

The unavailability of a sufficient number of wave probes to measure water elevation at more points around the structures meant that it was not possible to obtain information for wave characteristics at more points in the wave field, such as in the gap between the structures, in the middle of the platform and at their sides. Christou *et al* (2008), for example, used a moveable array of multiple wave probes to measure water elevation at various points around their models. This was not available to the researcher and so, also, due to time constraints, the decision was made to concentrate on wave measurements in front of and on the lee of the structures using the available probes.

➢ *Incomplete and limited view of the wave field*

Attempts to obtain images of the wave field, comprising a three-dimensional view of wave height, velocities, and locations around the structures, using particle image velocimetry (PIV) were unsuccessful due to the relatively large size of the tank, unfavorable lighting conditions for the camera and multiple reflections at the water surface. Stagonas and Müller (2006), for example, used PIV techniques to successfully map the wave fields in a smaller scale wave tank than the one used in this research. So, it was not possible to acquire direct overhead images of wave superposition to determine the precise nature and mechanism of superposition in the dissipation of wave energy, and only a limited view was obtained using the wave probes.

However, even with this limited view, it is this researcher's opinion that the probes provided enough data to allow some reasonable conclusions to be made of the energy dissipation behaviour of the model structures, as the basic idea is to measure the incident and transmitted wave heights and energy and to compare them for differences. This the wave probes were able to do.

V. RESULTS AND FINDINGS

A. Description of Display of Data

➢ *Arrangement of Tables and Graphs*

The processed data for incident wave height, wave periods, wavelengths, percentage changes in energy density, and loss coefficients are tabulated in Table 6 to Table 18 and illustrated graphically on bar charts in Figure 11 to Figure 23, containing the results of Exp. 1 to Exp. 13, respectively. The twelve selected wave conditions are numbered in each table as Wave Series (WS) 1 to 12 and are colour-coded in the bar charts so that each bar represents a change in energy density or a loss coefficient at a given wave probe. The results of each experiment are illustrated on two bar charts – (a) showing the percentage energy density changes and (b) showing the loss coefficients – as obtained from the wave probe data.

➢ *Percentage Energy Density Changes*

In the percentage energy density changes graphs, decreases in energy density are shown as negative values – bars below the horizontal axis, while increases in energy density as positive values – bars above the horizontal axis. In the case of the graphs of loss coefficients, only real number values of K_L are shown on the graphs - these occur when there is a decrease in energy density and a consequent real number loss coefficient according to Equation 3.16.

➢ *Loss Coefficients*

As discussed previously, any complex number value for loss coefficient, K_L, is denoted by an asterisk (*) in the tables since these are not real numbers. These would, however, indicate an increase in wave energy density. Average values of K_L for each wave series are shown in the tables, as well as an overall average K_L value for that particular type and arrangement of structure.

➢ *Wave periods and wavelengths*

For a given incident wave, the wave period did not change significantly after passing over the submerged structures, that this, the wave periods in front of the breakwaters were virtually the same as the periods in the lee. Hence, given that the depth was the same 0.15 m on both sides of the breakwaters, *d/L* was unchanged and so there were also no significant changes in wavelengths of a given incident wave. So only the incident wavelengths and wave heights are shown in the tables for each wave series.

B. Analysis of Data and Discussion

➢ *General Overview of Loss Coefficients and Changes in Wave Energy Density*

The results of Experiment 1 shown in Table 6 and Figure 11 indicate that the wave tank with no structure in it has the least energy-dissipative characteristics of the twelve wave series used. This is expected as the waves propagated freely with the least interference in the absence of obstacles in the tank. The overall average K_L for Experiment 1 was 0.11, which is the lowest average of all the wave experiments done. The corresponding overall average percentage energy density decrease is therefore -1.21 %, from Equation 3.17.

When the energy density data and loss coefficients of Experiment 1 are compared with the data from Experiments 2 – 13 in Tables 7 – 18, marked differences emerge. With the introduction of the structures in the wave tank, there is a noticeable change in the energy density in the lee of the structures with respect to the energy density in front as seen from Figures 12 – 23. All of the structures were able, to varying extents, to decrease the wave energy density as indicated by their increased loss coefficients and percentage energy density losses. For some wave series, the energy density increased, possibly due to local convergences or focusing of wave energy. The type and placement of structures seem to have varying effects on the wave energy

ISSN No:-2456-2165

density. These effects appear to depend also on the incident wave height and wavelength.

An overall perusal of the data given in the tables and the graphs indicates that, of the three types of structures, the planoconcave ones have the least energy dissipation characteristics, with overall average K_L values of 0.30, 0.25, 0.20, and 0.26 for Experiments 3, 6, 9 and 12, respectively. The planoconvex breakwaters have overall average K_L values of 0.33, 0.27, 0.30, and 0.30 for Experiments 2, 5, 8, and 11, respectively. The rectangular ones have overall average K_L values of 0.36, 0.35, 0.24, and 0.32, for Experiments 4, 7, 10, and 13, respectively. The rectangular ones seem to perform slightly better than the planoconvex in dissipating wave energy, but their performances are almost comparable.

One explanation for these differences in energy density and loss coefficient could be the bottom friction generated between the waves and the submerged platforms of the structures. Since the rectangular structures have the greatest platform areas of 0.0435 m^2, the planoconvex 0.0366 m^2, and the planoconcave 0.0243 m^2, the larger areas will cause more bottom friction, and hence, turbulence, which will extract energy from the waves. Hence, the planoconcave structures seem to dissipate the least energy, while the rectangular ones dissipate the most energy.

- *Effects of Structures on Waves*

The structures generally seem to produce better dissipation of energy density for longer and higher waves than for shorter and smaller waves, as seen from graphs in Figures 12 – 23. This would be an advantage since it is the longer and higher waves that have greater loadings and impacts on coastal structures (Smith *et al*, 1995). The smaller and short waves, as in Wave Series 10, 11, and 12, seem to pass over the structure with little impedance and even experienced a small increase in energy density in some cases.

For some wave series and structures, the change of energy density was not uniform across the wavefronts in the lee of the structures, and even the longer and higher waves (Wave Series 1 – 3) experienced an increase in energy density. This could be due to the wave-focusing effect of a single structure, or when two structures are used, to the presence of the gap of width, *a*, between two structures, as the waves passing over the gap can interact and superposition with those passing over the structures resulting in a convergence of wave energy in front of Wave Probe 3. Notably, this effect was seen in Exp. 2 (one planoconvex), Exp. 5 (two planoconvex, a = 0 cm), Exp. 3 (one planoconcave), Exp. 6 (two planoconcave, a = 0 cm); and Exp. 4 (one rectangular). This appears to be a case of wave focusing or convergence of wave energy. However, in the absence of a complete view of the wave field around the structures, it is not possible to come to a definite conclusion about the reason for the increase in energy density and the mechanism of wave energy focusing or convergence.

It is only possible to compare the energy density changes and loss coefficients of each structure and arrangement to assess which ones are better able to dissipate wave energy, on the bases of the data obtained.

Table 6: Experiment 1: No structures

Wave Series (WS)	**Incident Wave (Pr 1)**			**% Change energy density relative to Pr 1 (% ΔE)**			**Loss Coefficient K_L**			
	***H* (m)**	***L* (m)**	***H/L***	**Pr 2**	**Pr 3**	**Pr 4**	**Pr 2**	**Pr 3**	**Pr 4**	**Avg**
1	0.044	0.630	0.070	0.0	0.0	0.0	0.00	0.00	0.00	0.00
2	0.038	0.629	0.060	-5.2	0.0	-5.2	0.23	0.00	0.23	0.15
3	0.033	0.624	0.053	-11.8	0.0	-11.8	0.34	0.00	0.34	0.23
4	0.042	0.382	0.110	-9.3	-4.7	-18.1	0.30	0.22	0.43	0.32
5	0.034	0.382	0.089	0.0	0.0	-5.8	0.00	0.00	0.24	0.08
6	0.025	0.385	0.065	0.0	8.2	0.0	0.00	*	0.00	0.00
7	0.034	0.308	0.110	0.0	-5.8	-11.4	0.00	0.24	0.34	0.19
8	0.026	0.304	0.086	0.0	16.0	0.0	0.00	*	0.00	0.00
9	0.017	0.308	0.055	12.1	12.1	0.0	*	*	0.00	0.00
10	0.025	0.250	0.100	8.2	8.2	0.0	*	*	0.00	0.00
11	0.022	0.247	0.089	-8.9	9.3	-8.9	0.30	*	0.30	0.30
12	0.017	0.248	0.069	24.9	24.9	0.0	*	*	0.00	0.00
								Overall Avg		0.11

ISSN No:-2456-2165

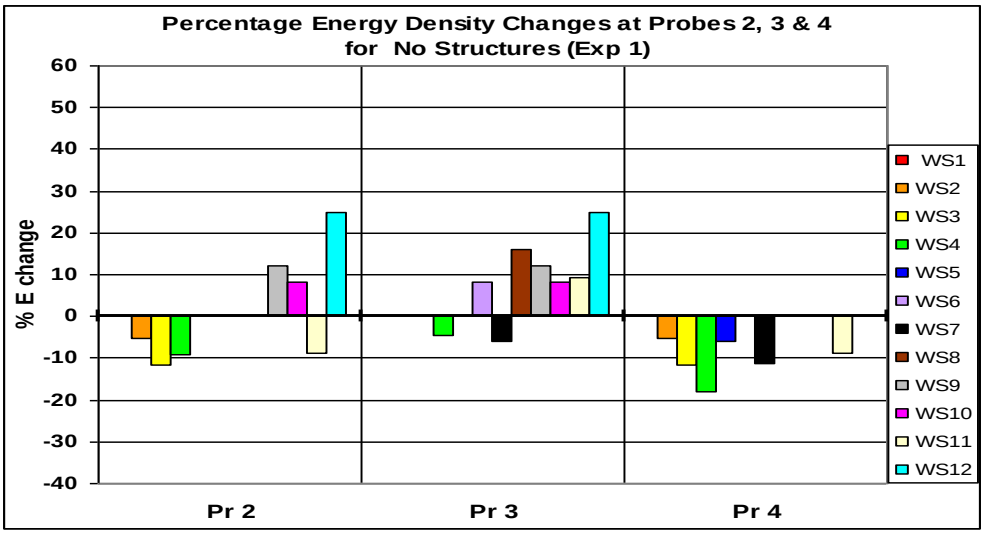

Fig. 11(a): Percentage Energy Density Changes for Exp. 1

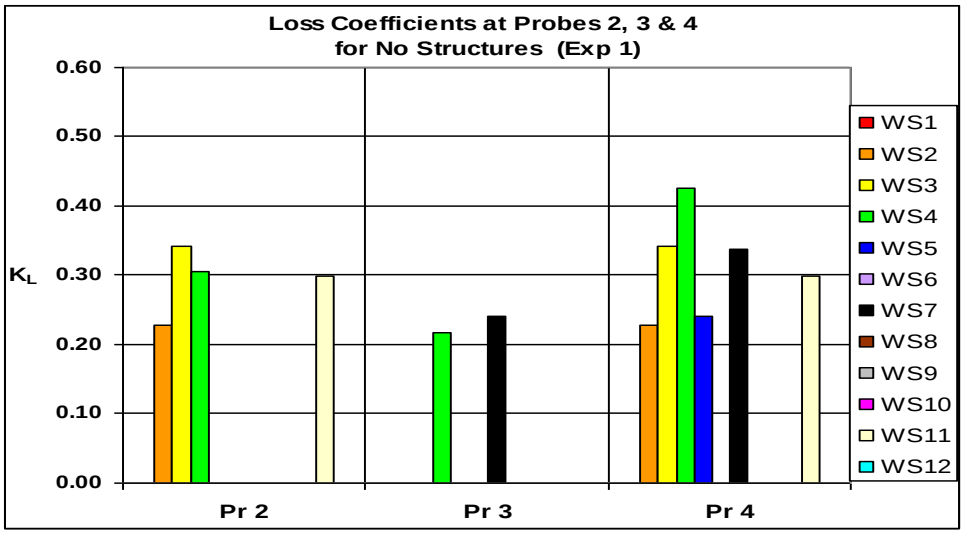

Fig.11(b): Loss Coefficients for Exp. 1

Table 7: Experiment 2: One Planoconvex

Wave Series (WS)	Incident Wave (Pr 1)			% Change energy density relative to Pr 1 (% ΔE)			Loss Coefficient K_L			
	H (m)	L (m)	H/L	Pr 2	Pr 3	Pr 4	Pr 2	Pr 3	Pr 4	Avg
1	0.045	0.630	0.071	-12.9	9.1	-12.9	0.36	*	0.36	0.36
2	0.040	0.626	0.064	-19.0	5.1	-14.4	0.44	*	0.38	0.41
3	0.033	0.620	0.053	-17.4	6.2	-17.4	0.42	*	0.42	0.42
4	0.045	0.382	0.118	-24.9	-21.0	-32.4	0.50	0.46	0.57	0.51
5	0.037	0.385	0.096	-15.6	0.0	-29.8	0.39	0.00	0.55	0.31
6	0.028	0.386	0.073	-26.5	7.3	-32.5	0.52	*	0.57	0.54
7	0.035	0.306	0.114	-5.6	-11.1	-16.4	0.24	0.33	0.41	0.33
8	0.027	0.305	0.089	-7.3	23.5	-14.3	0.27	*	0.38	0.32
9	0.017	0.306	0.056	0.0	38.4	-22.2	0.00	*	0.47	0.24
10	0.027	0.248	0.109	-7.3	0.0	-21.0	0.27	0.00	0.46	0.24
11	0.022	0.247	0.089	9.3	19.0	-8.9	*	*	0.30	0.30
12	0.017	0.247	0.069	12.1	38.4	0.0	*	*	0.00	0.00
								Overall Avg		**0.33**

ISSN No:-2456-2165

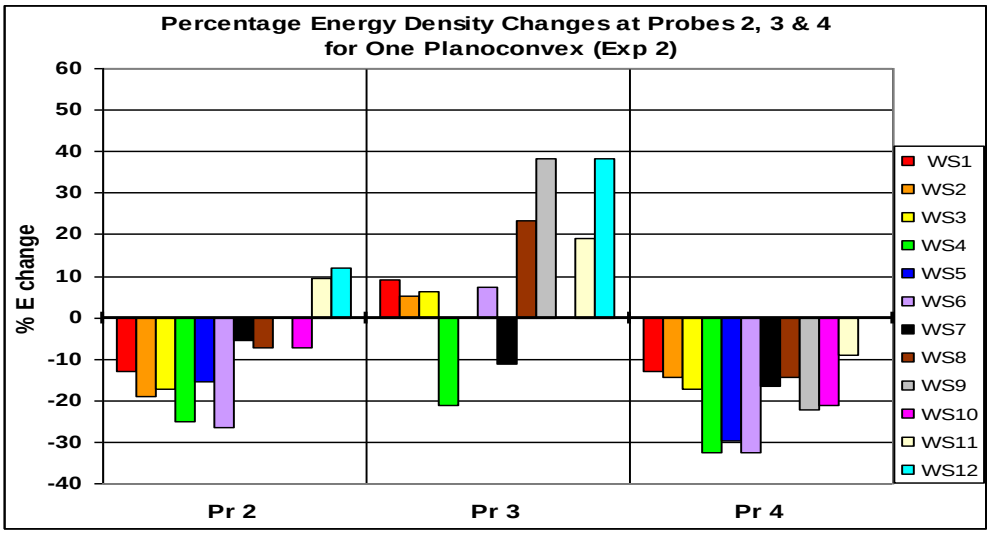

Fig. 12(a): Percentage Energy Density Changes for Exp. 2

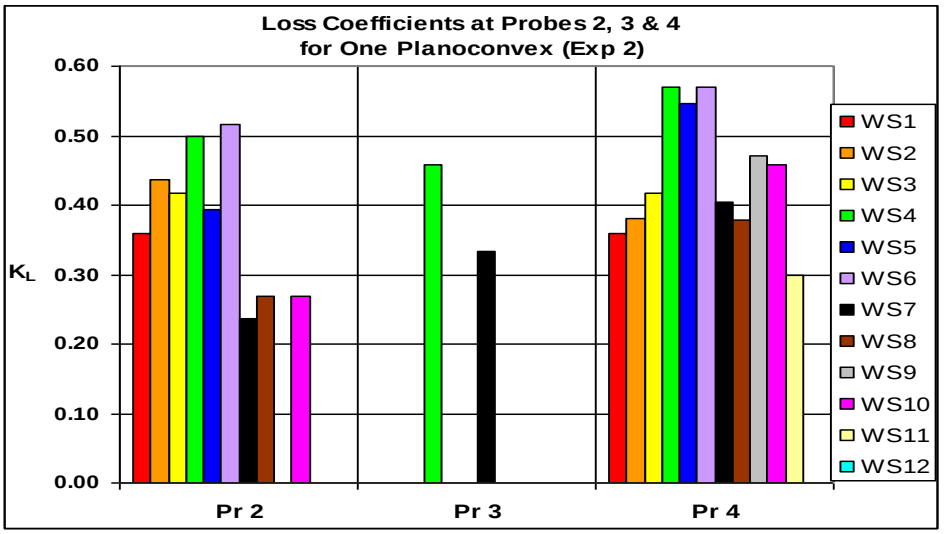

Fig. 12(b): Loss Coefficients for Exp. 2

Table 8: Experiment 3: One Planoconcave

Wave Series (WS)	**Incident Wave (Pr 1)**			**% Change energy density relative to Pr 1 (% ΔE)**			**Loss Coefficient K_L**			
	H **(m)**	***L*** **(m)**	***H/L***	**Pr 2**	**Pr 3**	**Pr 4**	**Pr 2**	**Pr 3**	**Pr 4**	**Avg**
1	0.043	0.632	0.068	-4.6	9.5	-9.1	0.21	*	0.30	0.26
2	0.038	0.623	0.061	-5.2	0.0	-5.2	0.23	0.00	0.23	0.15
3	0.032	0.624	0.051	-12.1	12.9	-12.1	0.35	*	0.35	0.35
4	0.043	0.380	0.113	-17.7	-17.7	-21.9	0.42	0.42	0.47	0.44
5	0.035	0.382	0.092	-5.6	5.8	-11.1	0.24	*	0.33	0.29
6	0.027	0.383	0.070	-14.3	0.0	-21.0	0.38	0.00	0.46	0.28
7	0.036	0.308	0.117	-10.8	-16.0	-16.0	0.33	0.40	0.40	0.38
8	0.027	0.306	0.088	-14.3	15.4	-14.3	0.38	*	0.38	0.38
9	0.017	0.309	0.055	-11.4	24.9	-11.4	0.34	*	0.34	0.34
10	0.026	0.248	0.105	-7.5	7.8	-7.5	0.27	*	0.27	0.27
11	0.022	0.246	0.089	0.0	9.3	-8.9	0.00	*	0.30	0.15
12	0.017	0.250	0.068	24.9	38.4	12.1	*	*	*	*
								Overall Avg		**0.30**

ISSN No:-2456-2165

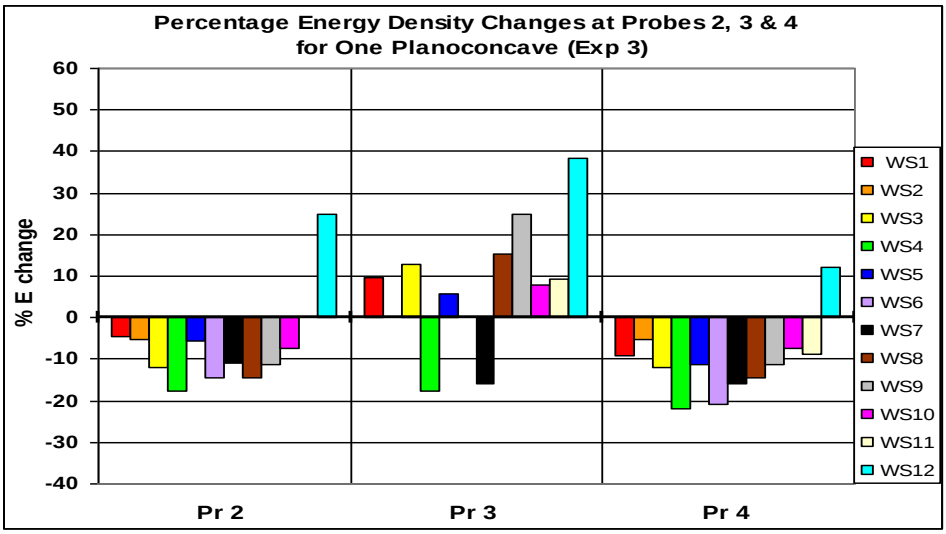

Fig. 13(a): Percentage Energy Density Changes for Exp. 3

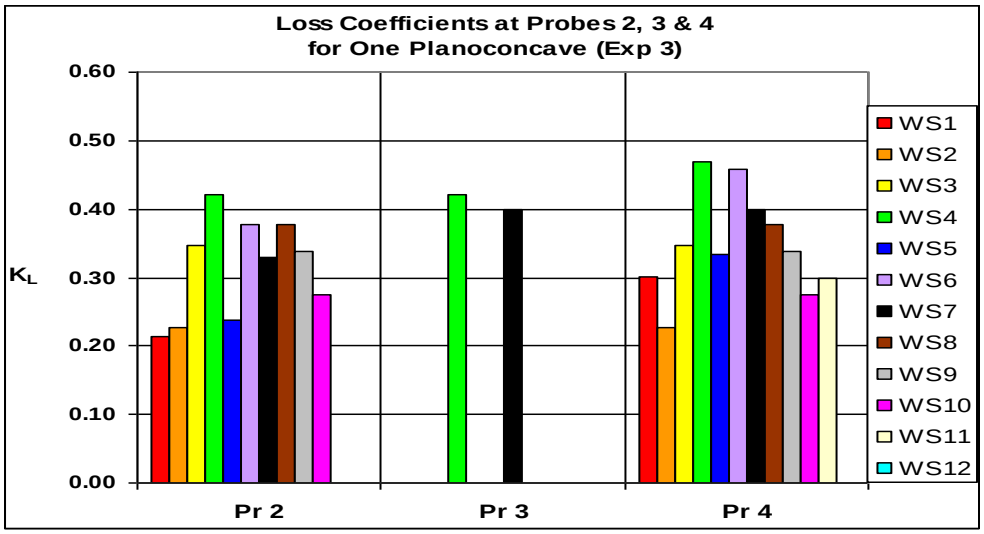

Fig. 13(b): Loss Coefficients for Exp. 3

Table 9: Experiment 4: One Rectangular

Wave Series (WS)	Incident Wave (Pr 1)			% Change energy density relative to Pr 1 (% ΔE)			Loss Coefficient K_L			
	H (m)	*L* (m)	*H/L*	Pr 2	Pr 3	Pr 4	Pr 2	Pr 3	Pr 4	Avg
1	0.046	0.629	0.073	-20.6	4.4	-12.6	0.45	*	0.36	0.40
2	0.040	0.627	0.064	-23.4	15.6	-14.4	0.48	*	0.38	0.43
3	0.034	0.623	0.055	-22.2	6.0	-16.9	0.47	*	0.41	0.44
4	0.045	0.386	0.117	-24.9	-28.7	-28.7	0.50	0.54	0.54	0.52
5	0.037	0.383	0.097	-20.5	0.0	-20.5	0.45	0.00	0.45	0.30
6	0.028	0.386	0.073	-26.5	7.3	-26.5	0.52	*	0.52	0.52
7	0.035	0.305	0.115	-5.6	-11.1	-11.1	0.24	0.33	0.33	0.30
8	0.027	0.308	0.088	-7.3	23.5	-14.3	0.27	*	0.38	0.32
9	0.017	0.308	0.055	-11.4	38.4	-11.4	0.34	*	0.34	0.34
10	0.026	0.250	0.104	-7.5	0.0	-7.5	0.27	0.00	0.27	0.18
11	0.022	0.246	0.089	0.0	19.0	-8.9	0.00	*	0.30	0.15
12	0.017	0.250	0.068	12.1	52.6	12.1	*	*	*	*
								Overall Avg		**0.36**

ISSN No:-2456-2165

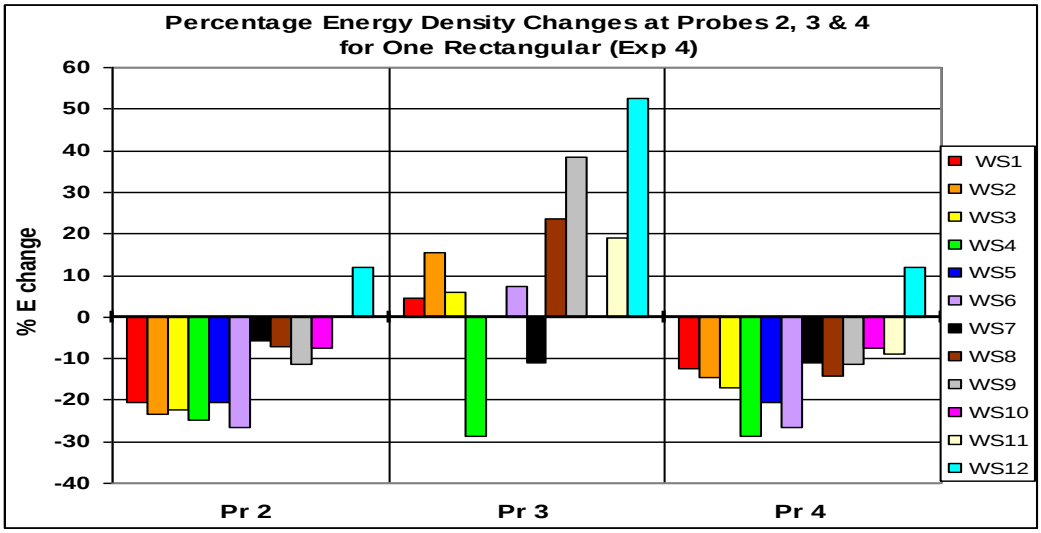

Fig. 14(a): Percentage Energy Density Changes for Exp. 4

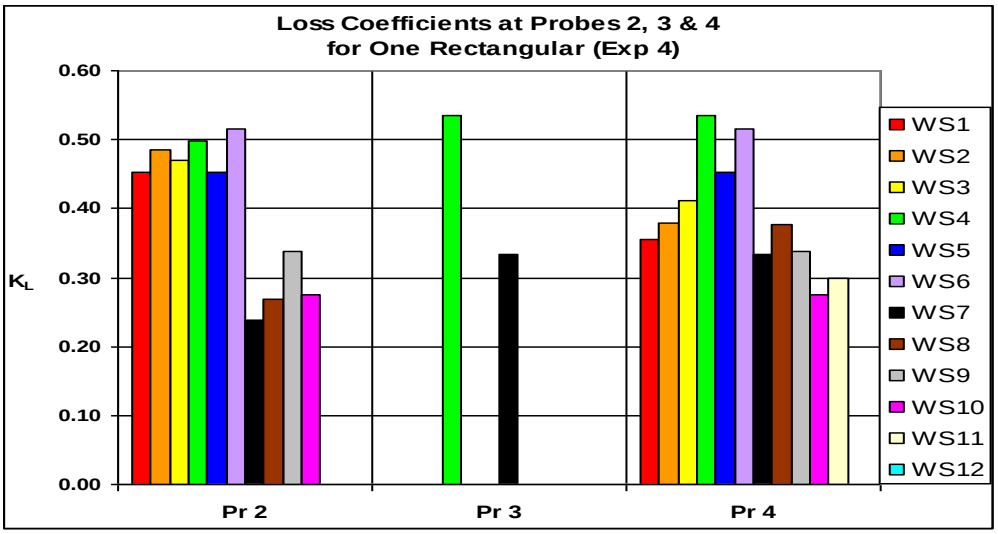

Fig. 14(b): Loss Coefficients for Exp. 4

Table 10: Experiment 5: Two Planoconvex, a = 0 cm

Wave Series (WS)	Incident Wave (Pr 1)			% Change energy density relative to Pr 1 (% ΔE)			Loss Coefficient K_L			
	H (m)	*L* (m)	*H/L*	Pr 2	Pr 3	Pr 4	Pr 2	Pr 3	Pr 4	Avg
1	0.045	0.626	0.072	-4.4	-4.4	-8.7	0.21	0.21	0.29	0.24
2	0.039	0.619	0.063	-10.0	5.2	-14.8	0.32	*	0.38	0.35
3	0.034	0.623	0.055	-22.2	0.0	-22.2	0.47	0.00	0.47	0.31
4	0.046	0.380	0.121	-28.1	-28.1	-31.8	0.53	0.53	0.56	0.54
5	0.037	0.383	0.097	-15.6	-5.3	-15.6	0.39	0.23	0.39	0.34
6	0.028	0.386	0.073	-13.8	7.3	-20.3	0.37	*	0.45	0.41
7	0.035	0.308	0.114	-16.4	-5.6	-21.6	0.41	0.24	0.46	0.37
8	0.026	0.311	0.084	7.8	24.4	-7.5	*	*	0.27	0.27
9	0.017	0.306	0.056	12.1	38.4	0.0	*	*	0.00	0.00
10	0.027	0.248	0.109	0.0	0.0	-7.3	0.00	0.00	0.27	0.09
11	0.022	0.246	0.089	9.3	19.0	0.0	*	*	0.00	0.00
12	0.017	0.250	0.068	38.4	52.6	24.9	*	*	*	*
								Overall Avg		**0.27**

ISSN No:-2456-2165

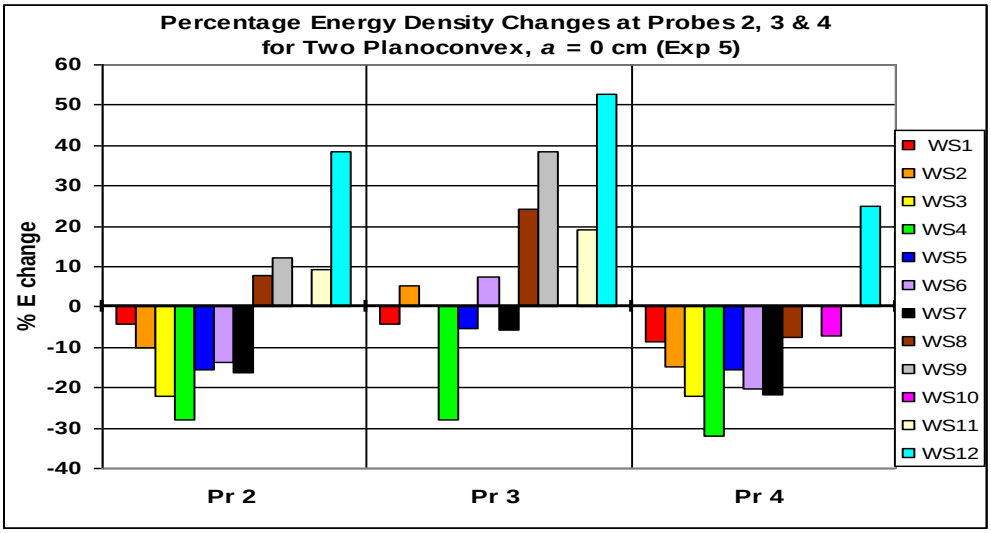

Fig. 15(a): Percentage Energy Density Changes for Exp. 5

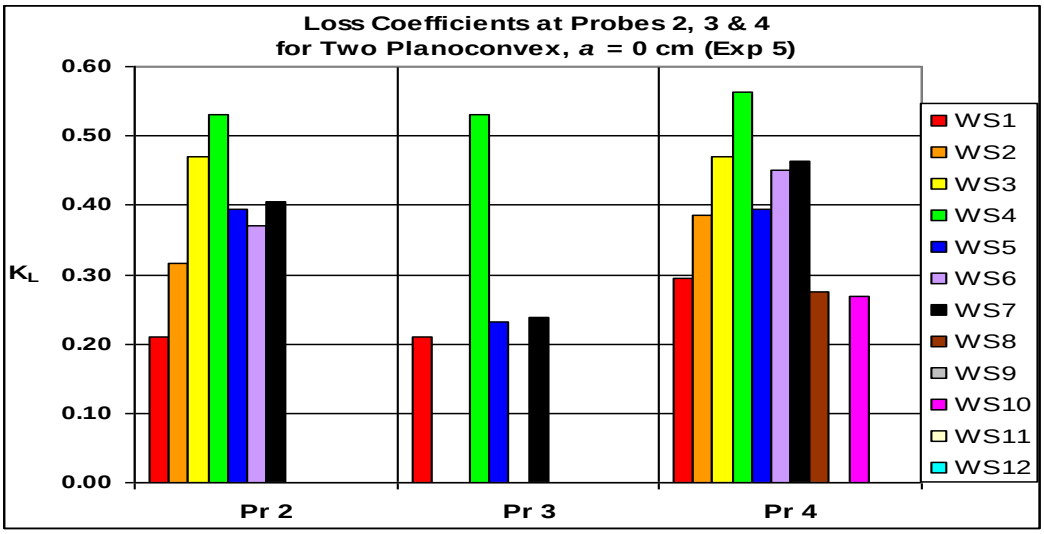

Fig. 15(b): Loss Coefficients for Exp. 5

Table 11: Experiment 6: Two Planoconcave, a = 0 cm

Wave Series (WS)	Incident Wave (Pr 1)			% Change energy density relative to Pr 1 (% ΔE)			Loss Coefficient K_L			
	H (m)	L (m)	H/L	Pr 2	Pr 3	Pr 4	Pr 2	Pr 3	Pr 4	Avg
1	0.045	0.632	0.071	-21.0	0.0	-12.9	0.46	0.00	0.36	0.27
2	0.039	0.632	0.062	-19.5	0.0	-14.8	0.44	0.00	0.38	0.28
3	0.033	0.626	0.053	-17.4	6.2	-11.8	0.42	*	0.34	0.38
4	0.043	0.380	0.113	-17.7	-17.7	-21.9	0.42	0.42	0.47	0.44
5	0.035	0.377	0.093	-5.6	5.8	-5.6	0.24	*	0.24	0.24
6	0.027	0.382	0.071	-14.3	0.0	-14.3	0.38	0.00	0.38	0.25
7	0.035	0.308	0.114	-11.1	-11.1	-11.1	0.33	0.33	0.33	0.33
8	0.027	0.311	0.087	-7.3	15.4	-7.3	0.27	*	0.27	0.27
9	0.017	0.306	0.056	12.1	38.4	0.0	*	*	0.00	0.00
10	0.026	0.248	0.105	0.0	0.0	0.0	0.00	0.00	0.00	0.00
11	0.022	0.247	0.089	9.3	9.3	9.3	*	*	*	*
12	0.018	0.250	0.072	11.4	23.5	11.4	*	*	*	*
								Overall Avg		**0.25**

ISSN No:-2456-2165

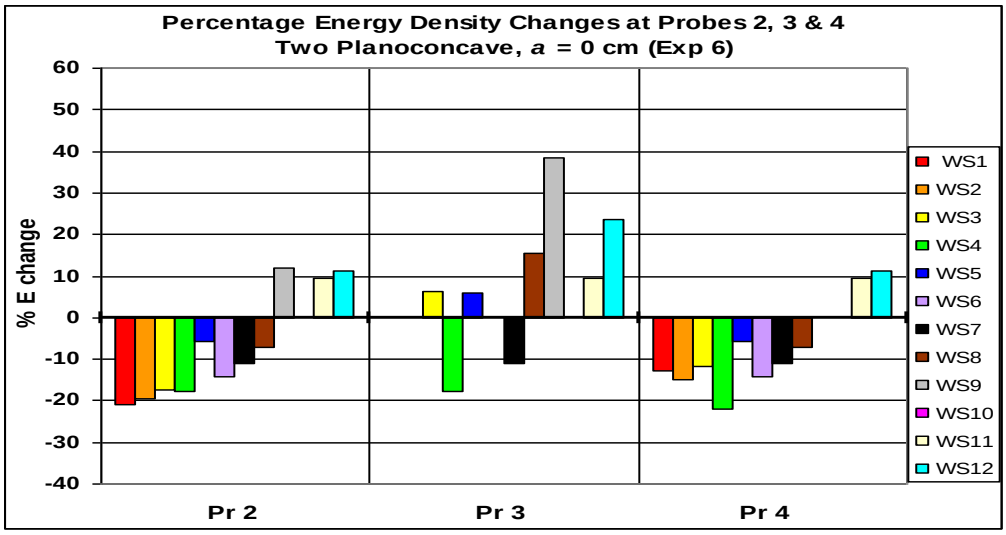

Fig. 16(a): Percentage Energy Density Changes for Exp. 6

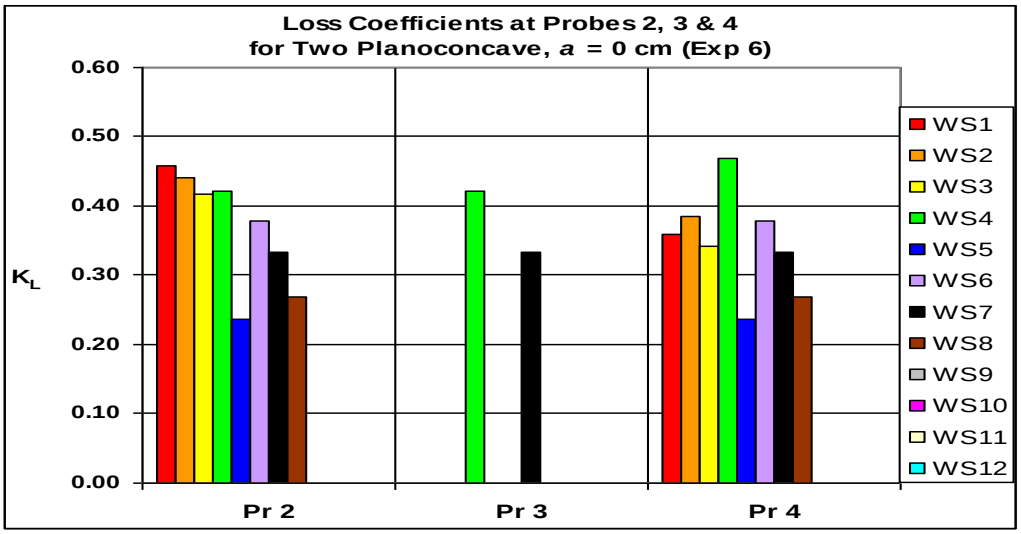

Fig. 16(b): Loss Coefficients for Exp. 6

Table 12: Experiment 7: Two Rectangular, a = 0 cm

Wave Series (WS)	Incident Wave (Pr 1)			% Change energy density relative to Pr 1 (% ΔE)			Loss Coefficient K_L			
	H (m)	L (m)	H/L	Pr 2	Pr 3	Pr 4	Pr 2	Pr 3	Pr 4	Avg
1	0.047	0.629	0.075	-16.3	-8.3	-16.3	0.40	0.29	0.40	0.37
2	0.041	0.626	0.065	-18.6	10.0	-18.6	0.43	*	0.43	0.43
3	0.036	0.623	0.058	-30.6	-5.5	-25.9	0.55	0.23	0.51	0.43
4	0.046	0.380	0.121	-28.1	-24.4	-28.1	0.53	0.49	0.53	0.52
5	0.038	0.385	0.099	-19.9	-10.3	-19.9	0.45	0.32	0.45	0.40
6	0.029	0.385	0.075	-19.6	-6.8	-19.6	0.44	0.26	0.44	0.38
7	0.035	0.308	0.114	-5.6	-5.6	-11.1	0.24	0.24	0.33	0.27
8	0.025	0.308	0.081	16.6	34.6	8.2	*	*	*	*
9	0.016	0.308	0.052	26.6	56.3	12.9	*	*	*	*
10	0.027	0.247	0.109	0.0	0.0	-7.3	0.00	0.00	0.27	0.09
11	0.024	0.245	0.098	-8.2	0.0	-16.0	0.29	0.00	0.40	0.23
12	0.018	0.247	0.073	23.5	36.1	11.4	*	*	*	*
								Overall Avg		**0.35**

ISSN No:-2456-2165

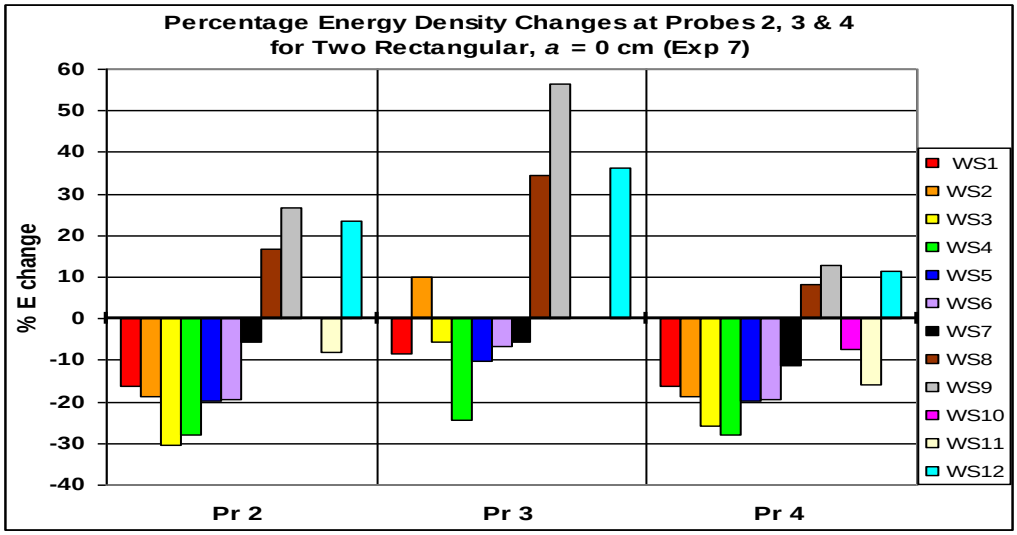

Fig. 17(a): Percentage Energy Density Changes for Exp. 7

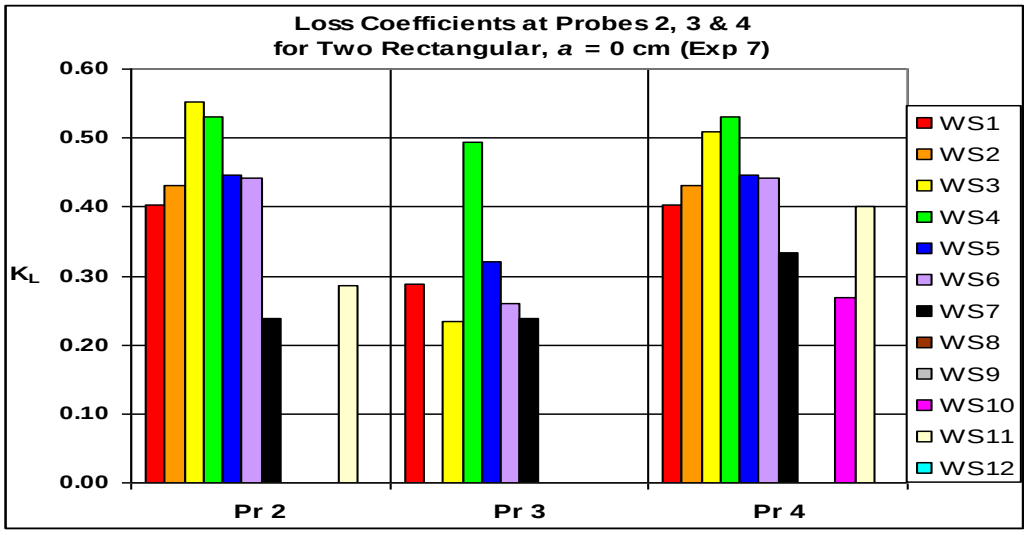

Fig. 17(b): Loss Coefficients for Exp. 7

Table 13: Experiment 8: Two Planoconvex, a = 7 cm

Wave Series (WS)	Incident Wave (Pr 1)			% Change energy density relative to Pr 1 (% ΔE)			Loss Coefficient K_L			
	H (m)	*L* (m)	*H/L*	Pr 2	Pr 3	Pr 4	Pr 2	Pr 3	Pr 4	Avg
1	0.051	0.630	0.081	-22.2	-22.2	-25.6	0.47	0.47	0.51	0.48
2	0.044	0.626	0.070	-21.4	-29.3	-25.4	0.46	0.54	0.50	0.50
3	0.038	0.624	0.061	-24.6	-29.1	-33.5	0.50	0.54	0.58	0.54
4	0.044	0.382	0.115	-29.3	-21.4	-25.4	0.54	0.46	0.50	0.50
5	0.036	0.383	0.094	-10.8	0.0	-10.8	0.33	0.00	0.33	0.22
6	0.027	0.385	0.070	0.0	-7.3	0.0	0.00	0.27	0.00	0.09
7	0.036	0.306	0.118	-21.0	-16.0	-16.0	0.46	0.40	0.40	0.42
8	0.027	0.306	0.088	7.5	7.5	0.0	*	*	0.00	0.00
9	0.017	0.305	0.056	12.1	24.9	12.1	*	*	*	*
10	0.027	0.250	0.108	7.5	-7.3	0.0	*	0.27	0.00	0.13
11	0.023	0.248	0.093	8.9	-8.5	0.0	*	0.29	0.00	0.15
12	0.018	0.247	0.073	11.4	23.5	11.4	*	*	*	*
								Overall Avg		0.30

ISSN No:-2456-2165

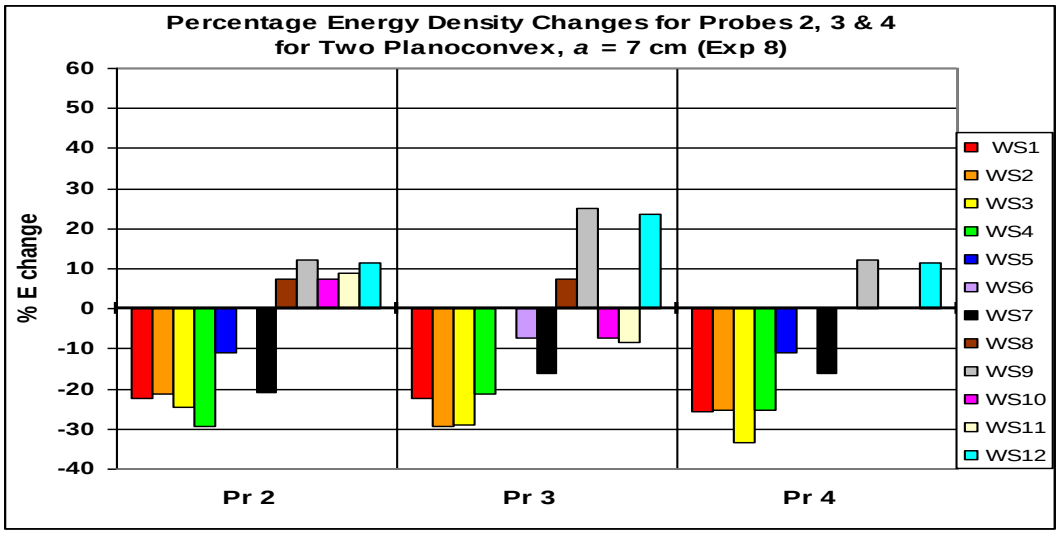

Fig. 18(a): Percentage Energy Density Changes for Exp. 8

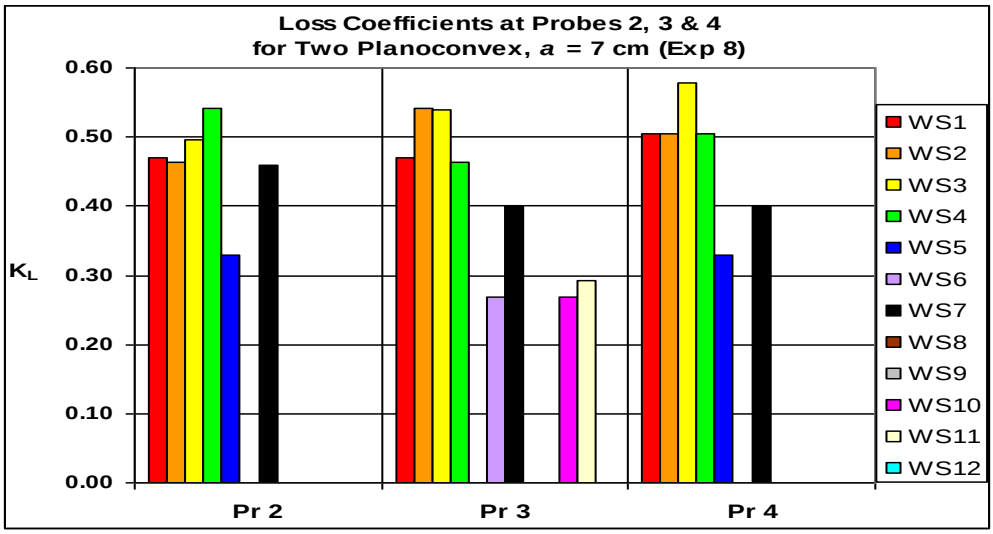

Fig. 18(b): Loss Coefficients for Exp. 8

Table 14: Experiment 9: Two Planoconcave, a = 7 cm

Wave Series (WS)	Incident Wave (Pr 1)			% Change energy density relative to Pr 1 (% ΔE)			Loss Coefficient K_L			
	H (m)	L (m)	H/L	Pr 2	Pr 3	Pr 4	Pr 2	Pr 3	Pr 4	Avg
1	0.046	0.629	0.073	-20.6	-8.5	-16.6	0.45	0.29	0.41	0.38
2	0.040	0.623	0.064	-23.4	-4.9	-23.4	0.48	0.22	0.48	0.40
3	0.034	0.623	0.055	-22.2	-5.8	-16.9	0.47	0.24	0.41	0.37
4	0.042	0.380	0.111	-18.1	-13.8	-18.1	0.43	0.37	0.43	0.41
5	0.034	0.382	0.089	0.0	0.0	0.0	0.00	0.00	0.00	0.00
6	0.026	0.383	0.068	-7.5	-7.5	0.0	0.27	0.27	0.00	0.18
7	0.035	0.306	0.114	-11.1	-16.4	-11.1	0.33	0.41	0.33	0.36
8	0.026	0.312	0.083	0.0	7.8	0.0	0.00	*	0.00	0.00
9	0.017	0.305	0.056	12.1	24.9	0.0	*	*	0.00	0.00
10	0.026	0.250	0.104	0.0	-7.5	0.0	0.00	0.27	0.00	0.09
11	0.022	0.247	0.089	9.3	9.3	0.0	*	*	0.00	0.00
12	0.017	0.248	0.069	24.9	24.9	12.1	*	*	*	*
								Overall Avg		**0.20**

ISSN No:-2456-2165

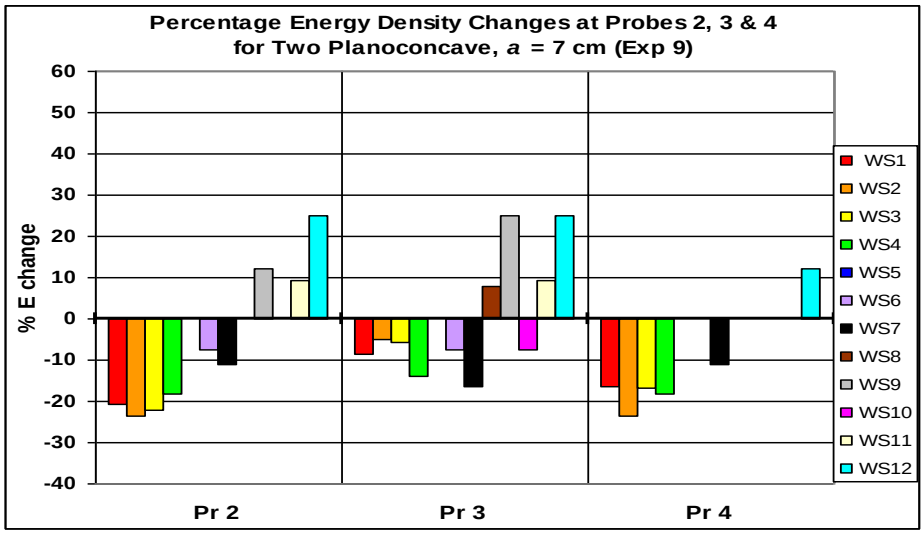

Fig. 19(a): Percentage Energy Density Changes for Exp. 9

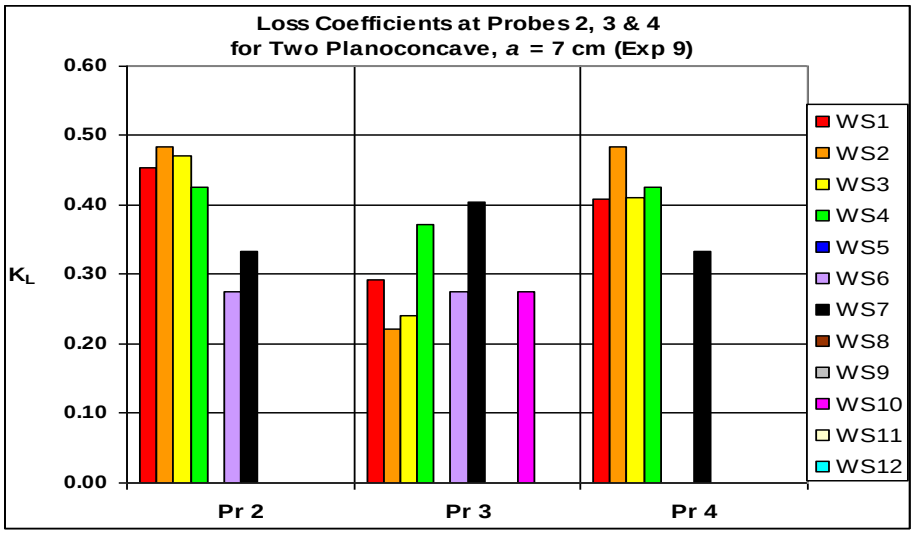

Fig. 19(b): Loss Coefficients for Exp. 9

Table 15: Experiment 10: Two Rectangular, a = 7 cm

Wave Series (WS)	Incident Wave (Pr 1)			% Change energy density relative to Pr 1 (% ΔE)			Loss Coefficient K_L			
	H (m)	L (m)	H/L	Pr 2	Pr 3	Pr 4	Pr 2	Pr 3	Pr 4	Avg
1	0.048	0.630	0.076	-23.4	-8.2	-16.0	0.48	0.29	0.40	0.39
2	0.040	0.630	0.063	-9.8	-4.9	-9.8	0.31	0.22	0.31	0.28
3	0.035	0.626	0.056	-21.6	0.0	-11.1	0.46	0.00	0.33	0.27
4	0.045	0.383	0.117	-24.9	-21.0	-28.7	0.50	0.46	0.54	0.50
5	0.037	0.385	0.096	-10.5	-10.5	-15.6	0.32	0.32	0.39	0.35
6	0.028	0.386	0.073	-7.0	-13.8	-7.0	0.26	0.37	0.26	0.30
7	0.034	0.307	0.111	-5.8	0.0	-5.8	0.24	0.00	0.24	0.16
8	0.027	0.305	0.089	7.5	0.0	7.5	*	0.00	*	0.00
9	0.017	0.308	0.055	12.1	24.9	12.1	*	*	*	*
10	0.027	0.248	0.109	0.0	-7.3	-7.3	0.00	0.27	0.27	0.18
11	0.023	0.247	0.093	0.0	0.0	0.0	0.00	0.00	0.00	0.00
12	0.018	0.250	0.072	23.5	23.5	11.4	*	*	*	*
								Overall Avg		0.24

ISSN No:-2456-2165

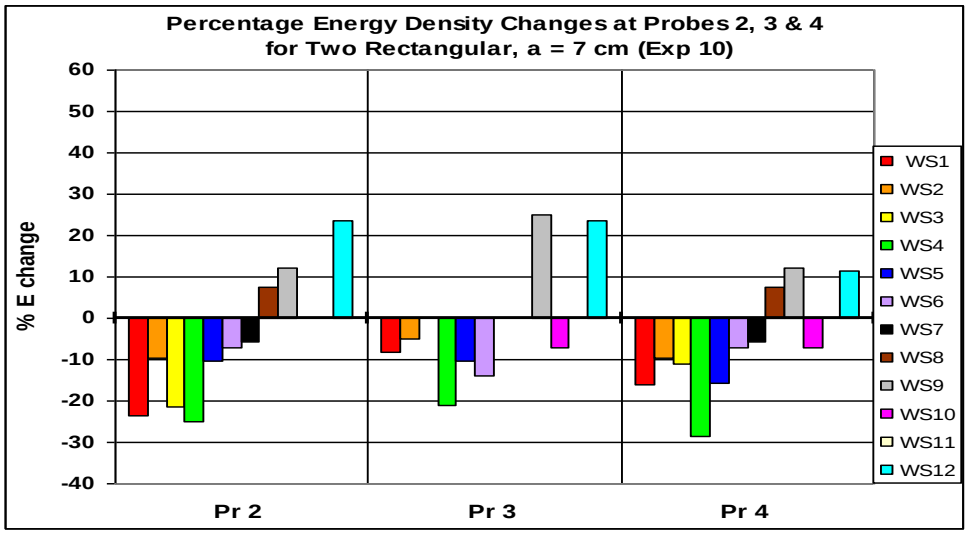

Fig. 20(a): Percentage Energy Density Changes for Exp. 10

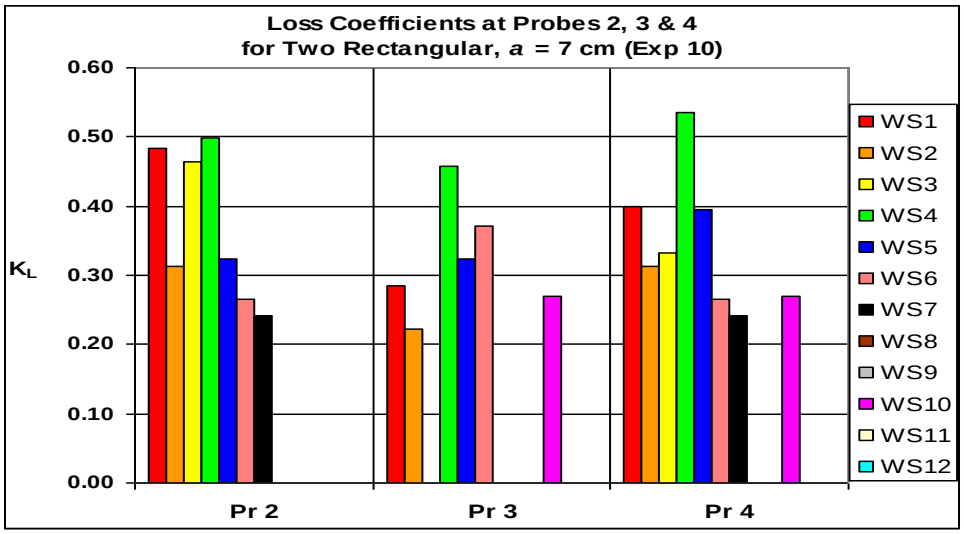

Fig. 20(b): Loss Coefficients for Exp. 10

Table 16: Experiment 11: Two Planoconvex, a = 14

Wave Series (WS)	Incident Wave (Pr 1)			% Change energy density relative to Pr 1 (% ΔE)			Loss Coefficient K_L			
	H (m)	L (m)	H/L	Pr 2	Pr 3	Pr 4	Pr 2	Pr 3	Pr 4	Avg
1	0.049	0.630	0.078	-23.0	-33.4	-19.4	0.48	0.58	0.44	0.50
2	0.043	0.626	0.069	-21.9	-26.0	-21.9	0.47	0.51	0.47	0.48
3	0.037	0.624	0.059	-25.2	-25.2	-29.8	0.50	0.50	0.55	0.52
4	0.043	0.382	0.113	-26.0	-21.9	-21.9	0.51	0.47	0.47	0.48
5	0.035	0.383	0.091	-5.6	-5.6	-5.6	0.24	0.24	0.24	0.24
6	0.027	0.386	0.070	0.0	-21.0	0.0	0.00	0.46	0.00	0.15
7	0.036	0.308	0.117	-16.0	-16.0	-16.0	0.40	0.40	0.40	0.40
8	0.027	0.306	0.088	7.5	0.0	0.0	*	0.00	0.00	0.00
9	0.017	0.305	0.056	12.1	12.1	12.1	*	*	*	*
10	0.026	0.248	0.105	16.0	-7.5	7.8	*	0.27	*	0.27
11	0.022	0.251	0.088	19.0	0.0	19.0	*	0.00	*	0.00
12	0.018	0.247	0.073	23.5	11.4	23.5	*	*	*	*
								Overall Avg		0.30

ISSN No:-2456-2165

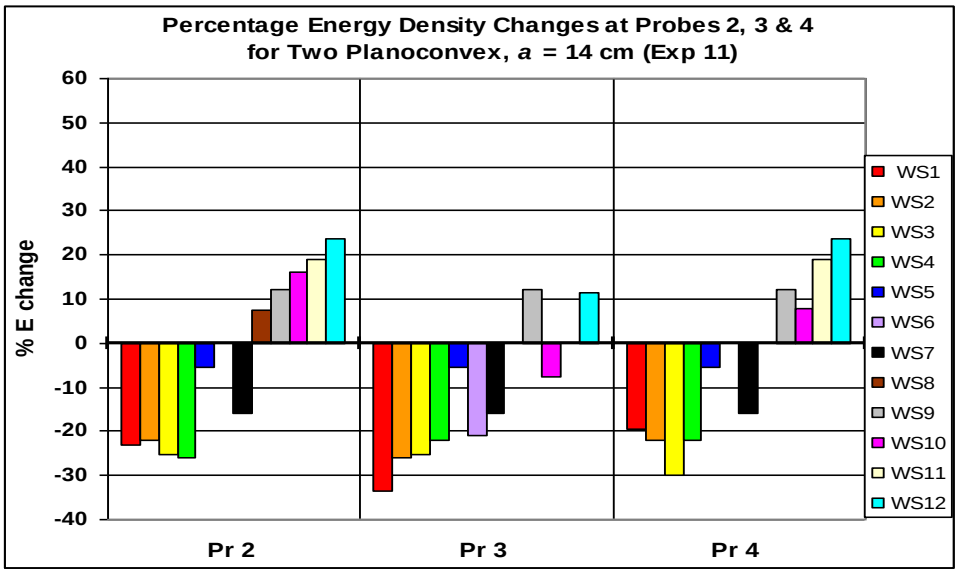

Fig. 21(a): Percentage Energy Density Changes for Exp. 11

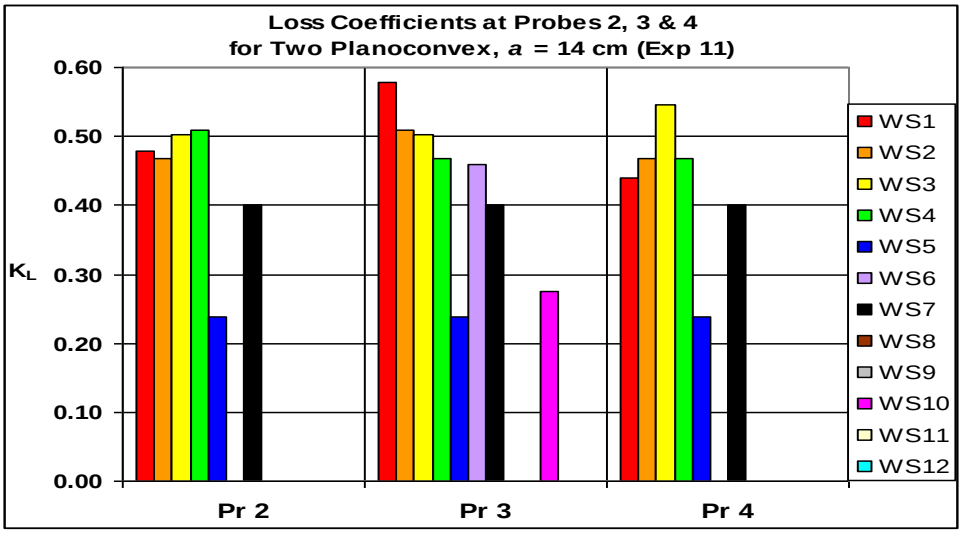

Fig. 21(b): Loss Coefficients for Exp. 11

Table 17: Experiment 12: Two Planoconcave, a = 14 cm

Wave Series (WS)	Incident Wave (Pr 1)			% Change energy density relative to Pr 1 (% ΔE)			Loss Coefficient K_L			
	H (m)	L (m)	H/L	Pr 2	Pr 3	Pr 4	Pr 2	Pr 3	Pr 4	Avg
1	0.047	0.629	0.075	-12.4	-20.1	-16.3	0.35	0.45	0.40	0.40
2	0.041	0.629	0.065	-18.6	-18.6	-22.9	0.43	0.43	0.48	0.45
3	0.036	0.618	0.058	-25.9	-30.6	-21.0	0.51	0.55	0.46	0.51
4	0.043	0.387	0.111	-26.0	-29.9	-33.8	0.51	0.55	0.58	0.55
5	0.035	0.386	0.091	-5.6	-11.1	-11.1	0.24	0.33	0.33	0.30
6	0.026	0.385	0.068	7.8	-7.5	0.0	*	0.27	0.00	0.14
7	0.035	0.306	0.114	-16.4	-11.1	-16.4	0.41	0.33	0.41	0.38
8	0.027	0.308	0.088	0.0	0.0	-7.3	0.00	0.00	0.27	0.09
9	0.017	0.308	0.055	12.1	12.1	0.0	*	*	0.00	0.00
10	0.025	0.250	0.100	8.2	0.0	0.0	*	0.00	0.00	0.00
11	0.022	0.247	0.089	0.0	0.0	0.0	0.00	0.00	0.00	0.00
12	0.017	0.248	0.069	12.1	24.9	12.1	*	*	*	*
								Overall Avg		0.26

ISSN No:-2456-2165

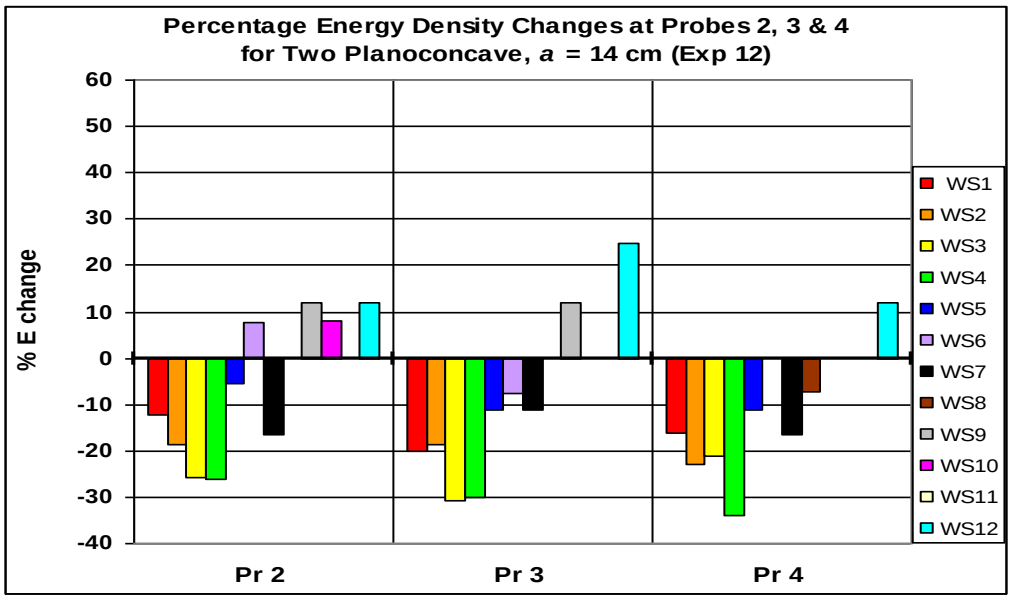

Fig. 22(a): Percentage Energy Density Changes for Exp. 12

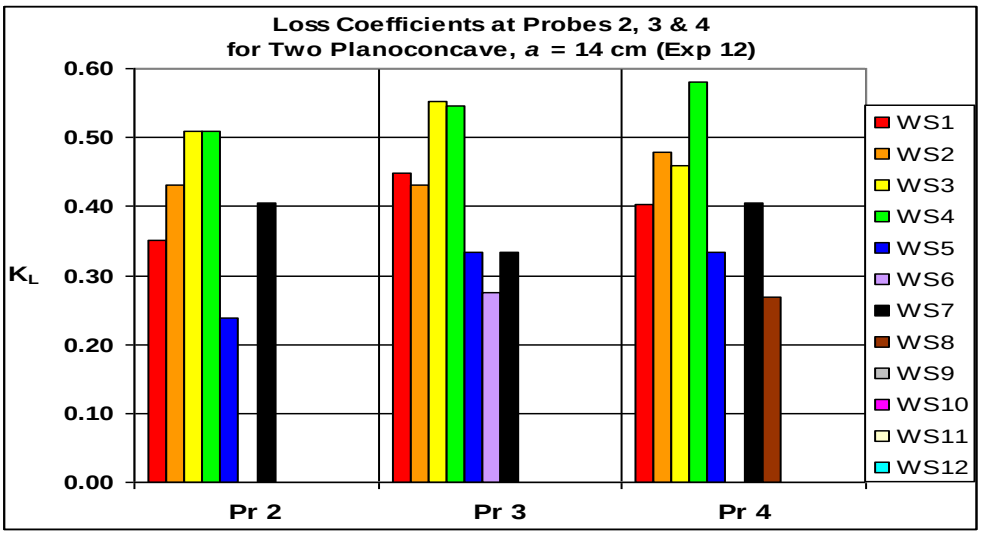

Fig. 22(b): Loss Coefficients for Exp. 12

Table 18: Experiment 13: Two Rectangular, a = 14 cm

Wave Series (WS)	Incident Wave (Pr 1)			% Change energy density relative to Pr 1 (% ΔE)			Loss Coefficient K_L			
	H (m)	L (m)	H/L	Pr 2	Pr 3	Pr 4	Pr 2	Pr 3	Pr 4	Avg
1	0.047	0.630	0.075	-31.2	-23.9	-20.1	0.56	0.49	0.45	0.50
2	0.041	0.629	0.065	-18.6	-14.1	-14.1	0.43	0.38	0.38	0.39
3	0.035	0.621	0.056	-21.6	-11.1	-16.4	0.46	0.33	0.41	0.40
4	0.043	0.382	0.113	-26.0	-26.0	-26.0	0.51	0.51	0.51	0.51
5	0.036	0.383	0.094	-5.5	-21.0	-10.8	0.23	0.46	0.33	0.34
6	0.027	0.386	0.070	7.5	-27.4	0.0	*	0.52	0.00	0.26
7	0.034	0.306	0.111	-11.4	-5.8	-11.4	0.34	0.24	0.34	0.31
8	0.025	0.306	0.082	16.6	8.2	25.4	*	*	*	*
9	0.016	0.304	0.053	26.6	12.9	26.6	*	*	*	*
10	0.026	0.252	0.103	7.8	-7.5	0.0	*	0.27	0.00	0.14
11	0.022	0.246	0.089	9.3	0.0	9.3	*	0.00	*	0.00
12	0.017	0.250	0.068	38.4	12.1	24.9	*	*	*	*
								Overall Avg		0.32

ISSN No:-2456-2165

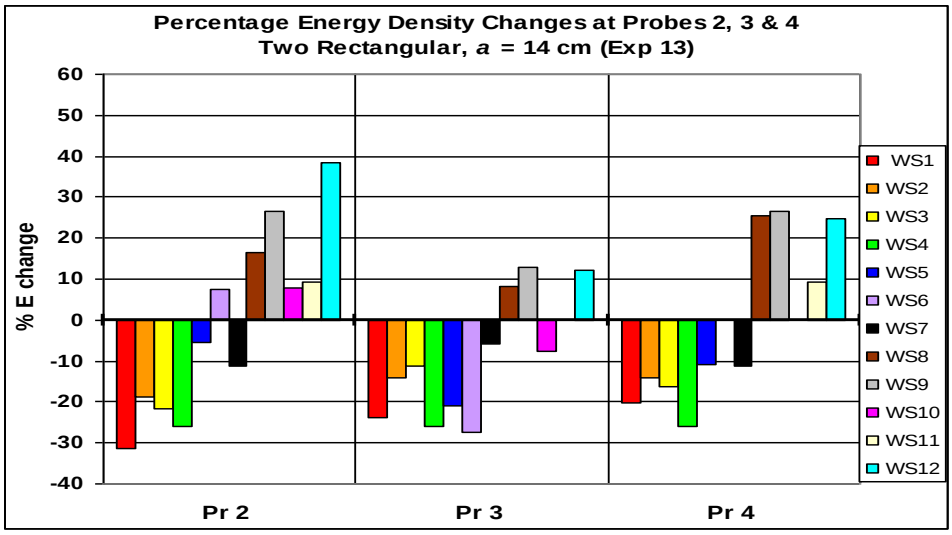

Fig. 23(a): Percentage Energy Density Changes for Exp. 13

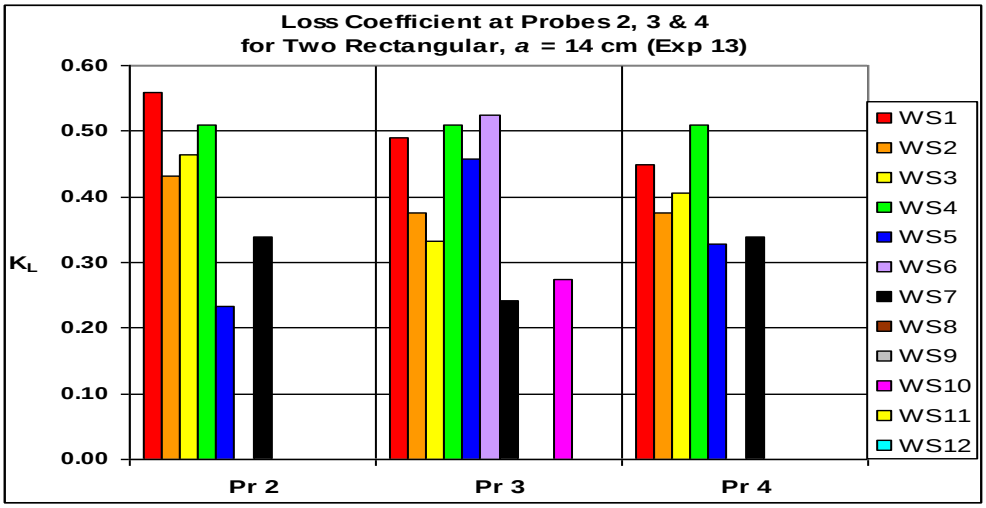

Fig. 23(b): Loss Coefficients for Exp. 13

➢ *Appearance of Breaker Lines Past Structures*

For all the structures, a line of small breakers, with the appearance of spilling breakers as described in the literature (Kamphuis, 2000; Reeve et al, 2004; Sorensen, 2006) was observed in the lee with Wave Series 1. This wave has a period of 0.67 s, wavelength 0.63 m, and incident wave heights ranging from 0.043 m (Exp.3) to 0.051 m (Exp.8). For this wave, H/L ≈ 0.07; H/d ≈ 0.3; d/L ≈ 0.24 (intermediate depth). These breakers appeared about 13 – 14 cm past the structures and disappeared just before reaching the three wave probes in the lee. This breaker line was not seen in the wave tank that had no structure in it (Experiment 1).

Evidently, it was the presence of the structures, and not their shape, that generated this spilling breaker due to the intermediate water platform depth, ds = 0.075 m relative to this particular wave height and wavelength. For this wave over the platform, L ≈ 0.51 m, H/L ≈ 0.09, H/ds ≈ 0.6, ds/L ≈ 0.148 (intermediate depth) and shoaling coefficient, Ks ≈ 0.92 (from Table 4). Given that the Miche limiting steepness for this wave over the structures is H/L ≈ 0.1 (Table 4), the wave broke because its steepness approached the limiting steepness. But due to the narrow crest width of the platform relative to the wavelength, the breaker line appeared past the structures, dissipated its energy, and then disappeared just in front of the lee side wave probes. Sorensen (2006) noted that only spilling and plunging breakers appear in deep water; but for the Wave Series 1, spilling breakers appeared in intermediate water depth, d/L ≈ 0.15 - 0.24.

Similar spilling breaker lines, but with smaller heights, were also seen for some of the other wave series in all the experiments. These breaker lines all developed between the structures and the lee side wave probes and faded away before reaching the probes. By observing the wave series in an experiment, it was noted that the height of the breakers and the intensity of breaking diminished going down the series. Only the experiments and waves series where these breaker lines appeared are shown in Table 19 From the d/L ratios it is seen that the water over the structures was of intermediate depth, while the H/d ratios indicate that the breaking criterion for shallow water waves was not reached by the waves. But the H/L ratio almost equaled and, in some cases, exceeded the Miche limiting wave steepness for intermediate depth. So, these waves experienced spilling breaking.

ISSN No:-2456-2165

Table 19: Experiments and wave series where small spilling breaker lines occurred in the lee of the structures.

Exp	WS	Waves over Structures			Miche Limit
		H/L	*H/d*	*d/L*	
2	1	0.089	0.600	0.148	0.104
2	2	0.079	0.533	0.148	0.104
2	4	0.131	0.600	0.219	0.125
2	10	0.113	0.360	0.313	0.137
2	11	0.092	0.293	0.313	0.137
3	1	0.085	0.573	0.148	0.104
3	2	0.075	0.507	0.148	0.104
3	4	0.125	0.573	0.219	0.125
3	10	0.108	0.347	0.313	0.137
3	11	0.092	0.293	0.313	0.137
4	1	0.091	0.613	0.148	0.104
4	2	0.079	0.533	0.148	0.104
4	4	0.131	0.600	0.219	0.125
4	5	0.108	0.493	0.219	0.125
4	7	0.122	0.467	0.262	0.132
4	10	0.108	0.347	0.313	0.137
4	11	0.092	0.293	0.313	0.137
5	1	0.089	0.600	0.148	0.104
5	2	0.077	0.520	0.148	0.104
5	4	0.134	0.613	0.219	0.125
5	5	0.108	0.493	0.219	0.125
5	7	0.122	0.467	0.262	0.132
5	10	0.113	0.360	0.313	0.137
5	11	0.092	0.293	0.313	0.137
6	1	0.089	0.600	0.148	0.104
6	4	0.125	0.573	0.219	0.125
6	7	0.122	0.467	0.262	0.132
6	11	0.092	0.293	0.313	0.137
7	1	0.093	0.627	0.148	0.104
7	2	0.081	0.547	0.148	0.104
7	4	0.134	0.613	0.219	0.125
7	7	0.122	0.467	0.262	0.132
7	10	0.113	0.360	0.313	0.137
8	1	0.101	0.680	0.148	0.104
8	2	0.087	0.587	0.148	0.104
8	4	0.128	0.587	0.219	0.125
8	7	0.126	0.480	0.262	0.132
8	10	0.113	0.360	0.313	0.137
8	11	0.096	0.307	0.313	0.137
9	1	0.091	0.613	0.148	0.104
9	4	0.122	0.560	0.219	0.125
9	7	0.122	0.467	0.262	0.132
9	10	0.108	0.347	0.313	0.137
9	11	0.092	0.293	0.313	0.137
10	1	0.095	0.640	0.148	0.104
10	2	0.079	0.533	0.148	0.104
10	4	0.131	0.600	0.219	0.125
10	7	0.119	0.453	0.262	0.132
10	10	0.113	0.360	0.313	0.137
10	11	0.096	0.307	0.313	0.137
11	1	0.097	0.653	0.148	0.104
11	2	0.085	0.573	0.148	0.104
11	3	0.073	0.493	0.148	0.104
11	4	0.125	0.573	0.219	0.125
11	5	0.102	0.467	0.219	0.125
11	10	0.108	0.347	0.313	0.137
11	11	0.092	0.293	0.313	0.137
12	1	0.093	0.627	0.148	0.104
12	4	0.125	0.573	0.219	0.125
12	7	0.122	0.467	0.262	0.132
12	10	0.104	0.333	0.313	0.137
13	1	0.093	0.627	0.148	0.104
13	2	0.081	0.547	0.148	0.104
13	4	0.125	0.573	0.219	0.125
13	7	0.119	0.453	0.262	0.132
13	11	0.092	0.293	0.313	0.137
7	11	0.100	0.320	0.313	0.137

The experiments and wave series in which this kind of breaking occurred corresponded closely with those where loss coefficients and percentage energy losses were highest. This indicated that wave breaking, caused by the structures, was one of the mechanisms of energy dissipation as noted in the literature (e.g., Reeve *et al*, 2004; Sorensen, 2006). Again, it is seen that the planoconcave structures induced less breaking than the other two, while the planoconvex and the rectangular structures performed comparably in causing breaking.

- *Effect of Gap Width, a, on Energy Changes*

The size of the gap width, *a*, between the structures seems to play a small part in energy dissipation, but this cannot be readily concluded. In the case of the two planoconvex structures where *a* = 0 cm (Table 10, Fig. 15, Exp. 5), the energy density increased as measured by Probe

ISSN No:-2456-2165

3 but decreased as measured by Probes 2 and 4 for six wave series. This appeared to be a focusing or convergence effect. For the planoconvex with the larger gaps, a = 7 cm, and 14 cm, (Exp. 8 & Exp.11) there is a more uniform decrease of energy density, with the performance of both in dissipating energy almost the same. Similar observations are made of the gap widths with the two planoconcave and two rectangular structures: the absence of a gap seems to increase the energy density, while its presence decreases energy density. As mentioned earlier, this could be due to the superposition of waves passing over the gap and over the structures, resulting in focusing of energy in the lee of the structures. But this cannot be definitely concluded without knowledge of the complete wave field around the structures.

- *Grading the Energy Dissipation Performance of the Structures*

Using the overall average loss coefficients in Tables 7 – 18 and the bar charts in Figures 12 – 23, the structures and arrangements are ranked in order of increasing energy dissipation performance as seen in Table 20.

Table 20: Ranked energy dissipation performance of structures

Exp	Structure	Gap width (cm)	Overall avg K_L	Overall avg % ΔE
9	2 planoconcave	7	0.20	- 4.0
10	2 rectangular	7	0.24	- 5.8
6	2 planoconcave	0	0.25	- 6.3
12	2 planoconcave	14	0.26	- 6.8
5	2 planoconvex	0	0.27	- 7.3
3	1 planoconcave	nil	0.30	- 9.0
11	2 planoconvex	14	0.30	- 9.0
8	2 planoconvex	7	0.30	- 9.0
13	2 rectangular	14	0.32	-10.2
2	1 planoconvex	nil	0.33	-10.9
7	2 rectangular	0	0.35	-12.3
4	1 rectangular	nil	0.36	-13.0

VI. CONCLUSIONS

The water elevation levels in front of and on the lee of the submerged structures were measured by the wave probes to obtain a time history of the wave heights at those points in the wave field around the structures. From the wave heights versus time graphs, the wave periods, wave heights, and wavelengths were determined. The wave energy density in front of the submerged structures and on their lee was then calculated and the energy differences between the two points were determined. The energy loss coefficient for waves passing over the structures was determined from the transmission coefficient, which was found from the incident and transmitted wave heights. These measured quantities were used to compare the energy dissipation characteristics of the three structures and their arrangement for the twelve selected wave conditions.

All of the structures were able to dissipate wave energy to varying extents. Generally, they dissipated the energy of the longer high amplitude waves better than the energy of the shorter low amplitude waves, confirming the report in the literature on submerged breakwaters (e.g., Smith et al, 1995; Neelamani & Rajendran, 2000). The rectangular structures showed the best energy dissipative characteristics for the wave conditions used. These were followed closely by the planoconvex structures which showed comparable energy dissipative performance. The planoconcave structures had the least energy dissipative effect but were still able to attenuate some of the wave energy when compared to the tank with no structure in it.

The planoconcave structures did not perform as well as was expected, that is, to reduce the wave energy by diverging and spreading out the incident wave energy, causing the energy density to be lowered. Nevertheless, they did exhibit some energy dissipative characteristics.

The planoconvex structures showed much promise when compared to the regular rectangular submerged breakwaters as their energy dissipation characteristics compared favorably with the rectangular ones. This is a key finding and could serve as a springboard for future investigations into curved planform submerged breakwaters.

The effects of the gap between structures on wave energy dissipations were not readily evident, although the smaller 7 cm gap does seem to induce better energy dissipation than the larger 14 cm gap, while no gap seems to be associated with energy density increase. In the absence of a complete view of the wave field, the energy dissipating or focusing mechanism of the gap remains unclear.

The mechanisms for energy dissipation in the lee of the breakwaters appear to be bottom friction between the submerged plan surface area of the structures and wave breaking caused by the intermediate relative water depth over the structures. The larger surface area of the rectangular structure possibly induced more bottom friction and energy dissipation than the smaller surface areas of the other two structures.

Superposition due to refractive wave focusing, convergence, and divergence may have also played a role in dissipating energy by causing wave heights to increase until the breaking criteria were reached. However, due to the very limited view of the wave field, it was not possible to determine for certain the involvement and mechanism of superposition in energy dissipation. This aspect of the study therefore remains inconclusive and so there is scope for further research in the future.

VII. RECOMMENDATIONS

A. Coastal Protection

The plano-convex structure would be more economical than the rectangular one to construct as it saves on costs and building materials and performs comparably to the rectangular breakwater in dissipating wave energy. With the models used in this research, the surface area of the planoconvex shape is 16 % smaller than the rectangular shape, and the planoconcave's surface area is 44 % smaller. This could mean a possible saving of 16 % – 40 % in building materials in a full-scale structure with a reduction in energy density comparable to the regular rectangular submerged breakwaters.

The smaller gap should be present between the two planoconvex structures, as this arrangement seems to dissipate more energy than the ones with the larger gap, whereas a zero gap seems to concentrate and increase the energy density for some wave conditions.

McCormick (1981) has suggested that these kinds of structures can be readily built using cofferdams filled with stone, rubble, grout, or reinforced concrete and faced with sheet pilings.

If these concave and convex shapes occur naturally in the sea near coastal structures, they can affect wave transmission over them and cause focusing of wave energy on land and shore structures under certain wave conditions. Coastal engineers will have to take them into account when designing coastal structures near such submerged features.

When introducing artificial submerged features near the coast, engineers should ensure that wave focusing is not directed unto coastal structures, unless that is the design intention for wave energy conversion devices. Attention needs to be paid to the wave climates, as the submerged feature might focus a particular wavelength unto a shore structure and place detrimental loadings on it.

B. Further Research

A greater variety and arrangement of structures and shapes with varying radii of curvature can be investigated. For example, biconvex and biconcave structures, that is, structures that are curved on both sides, can be studied. The double curvature will have a better refractive and focusing effect than the single curved surface as used in this research (McCormick, 1981). Varying the radius of curvature of the shapes will make the focal distance vary and so cause the focal point of waves to shift, as seen from the lens-maker equation (3.1 & 3.2)

The use of video photography involving particle image velocimetry is recommended to acquire the overall wave field in front of and on the lee of the structures. This will help to determine the precise mechanism that involves refraction and superposition in the dissipation of energy. The PIV, in particular, will need good and controlled lighting conditions, especially when using a fairly large wave tank.

A greater variety of wave conditions with regard to wavelengths and wave heights in different water depths can be used to test the energy dissipative behaviour of the structures across a wider wave spectrum. This will give a better understanding of the wave refraction, focusing, and dissipation characteristics of the structures under a variety of wave conditions.

A moveable array of multiple wave probes would be very useful in measuring water elevations at various points around the structures to give a rapid and accurate test of wave heights and energy density.

This researcher hopes that this study will serve as an impetus for the further investigation of submerged curved planform breakwaters as a means of coastal protection.

ACKNOWLEDGEMENTS

The author extends thanks to the following persons from the University of Southampton for giving advice and guidance and assisting in this research project:

Prof. Carl Amos, National Oceanography Centre
Dr. Derek Clarke, School of Civil Engineering and the Environment
Dr. Gerald Müller, School of Civil Engineering and the Environment
Davide Magagna, School of Civil Engineering and the Environment
Dmitris Stagonas, School of Civil Engineering and the Environment
David Warbrick, School of Civil Engineering and the Environment

The author also thanks the University of Southampton for the Hydraulics laboratory facilities and for providing all the necessary technical support.

Finally, thanks to Ms. Ashmini Prasad, English Assistant Mistress of the Tagore Memorial Secondary School, Guyana, for motivation and encouragement in completing this manuscript and proofreading the non-technical parts of it.

REFERENCES

[1.] Armfield Engineering Education. 2006. Hydraulics Research Instruments: Wave Probe System. http://www.armfield.co.uk/h40_datasheet.html. On 25 August 2008.
[2.] Chaplain, J. 2008. Wave Transformations Lecture Notes. School of Civil Engineering and the Environment, University of Southampton.

[3.] Cheng S., Liu, S., and Zheng, Y. 2003. Application study on submerged breakwaters used for coastal protection. International Conference on Estuaries and Coasts, November 2003, Hangzhou, China.
[4.] Cho, Y.-S., Jeon, C.-H., Lee, J.-I., and Lee, B.-H. 2006. Strong reflection of sinusoidal waves due to trapezoidal submerged porous breakwaters. Proceedings of the 8th International Coastal Symposium, Brazil. Journal of Coastal Research, SI 39, 838-841.
[5.] Christou, M., Swan, C., and Gudmestad, O. T. 2008. The interaction of surface water waves with submerged breakwaters. Coastal Engineering 55, 945-958.
[6.] Coastal Wiki. December 2008. Application of Breakwaters. Flanders Marine Institute (VLIZ), Belgium.
[7.] http://www.coastalwiki.org/coastalwiki/Application_of_breakwaters. On 20 June 2009.
[8.] Dean, R., and Dalrymple, R. 1991. Water wave mechanics for engineers and scientists. World Scientific Publishing Co. Pte. Ltd., Singapore.
[9.] Engineering Research News: Research Highlights. February 1996. Coastal Protection by Submerged Plate Breakwater.
[10.] http://www.eng.nus.edu.sg/EResnews/9602/feb96p8a.html. On 17 June 2009.
[11.] Halliday, D., Resnick, R., and Krane, K. 1992 (4th Edition). Physics (Volume 2). John Wiley & Son, Inc., New York.
[12.] Hung, C.-W., Chen, H.-B., and Tsai, C.-P. 2008. Simulation of shoreline change behind a submerged permeable breakwater. Taiwan-Polish Joint Seminar on Coastal Protection, November 2008, Tainan, Taiwan.
[13.] Kamphuis, W. 2000. Introduction to coastal engineering and management. World Scientific Publishing Co. Pte. Ltd., Singapore.
[14.] Losada, I. J., Silva, R., and Losada, M. A. 1996. 3-D non-breaking regular wave interaction with submerged breakwaters. Coastal Engineering 28, 229 – 248.
[15.] McCormick, M. E., 1981. Ocean Wave Energy Conversion. John Wiley & Sons, Inc., New York.
[16.] Mehlum, E., and Stamnes. J. 1979. “On the Focusing of Ocean Swells and Its Significance in Power Production,” Symposium on Wave Energy Utilization, Chalmers University, Gothenburg, Sweden.
[17.] Müller, G. 2008. Individual design project: Pre-feasibility study new Alderney Breakwater. School of Civil Engineering and the Environment, University of Southampton.
[18.] Neelamani, S. and Rajendran, R. 2000. Wave interaction with T-type breakwaters. Ocean Engineering 29 (2002) 151–175.
[19.] Nelkon, M. 1978 (6th Edition). Optics, Waves, and Sound. Heinemann Educational Books Ltd, London.
[20.] Priya, M. S. K., Sekhar, K. A. R., Sundar, V., Vadivelu, R. S., and Graw, K.-U. 2000. Dynamic pressures exerted on submerged semicircular breakwaters. ICOPMAS 2000, 4th International Conference on Coasts, Ports and Marine Structures, November 2000, Bandar Abbas, Iran.
[21.] Reeve, D., Chadwick, A., and Fleming, C. 2004. Coastal engineering: processes, theory and design practices. Spon Press Taylor & Francis Group, London.
[22.] Smith, D., Warner, P., Sorenson, R., Nurse, L., and Atherley, K. 1995. Submerged-crest breakwater design. Proceedings of the international conference of the Institution of Civil Engineers, April 1995, London. In Advances in coastal structures and breakwaters, pp 209-219.
[23.] Sorensen, R. M. 2006 (3rd Edition). Basic Coastal Engineering. Springer Science + Business Media, LLC, New York.
[24.] Stagonas, D., and Müller, G. 2006. Wave field mapping with particle image velocimetry. Ocean Engineering 34 (2007) 1781-1785.
[25.] Stauble, D., and Tabar, J. 2003. The use of submerged narrow-crested breakwaters for shoreline erosion control. Journal of Coastal Research 19(3), 684-722.
[26.] Zhu, S., Zhao, G., and Ma, Y. 2002. Hydraulic behaviour of a submerged perforated breakwater. 15th ASCE Engineering Mechanics Conference, June 2002, New York. EM 2002.